

AD A091756

AVRADCOM  
Report No. TR 80-F-9

**LEVEL**

AD

MANUFACTURING METHODS AND TECHNOLOGY  
(MANTECH) PROGRAM

SERVICE LIFE DETERMINATION FOR THE UH-60A (UTTAS)  
HELICOPTER ELASTOMERIC BEARINGS

Ernest P. Gaudette  
Lord Kinematics  
1635 W. 12th Street  
Erie, Pennsylvania, 16512

DTIC

SELECTED

NOV 14 1980

C

FINAL REPORT

April 1980

Contract No. DAAG46-78-C-0030



Approved for public release;  
distribution unlimited

United States Army  
AVIATION RESEARCH AND DEVELOPMENT COMMAND

ADG FILE COPY

80 11 10 071

The findings in this report are not to be construed as an official Department of the Army position, unless so designated by other authorized documents.

Mention of any trade names or manufacturers in this report shall not be construed as advertising nor as an official indorsement or approval of such products or companies by the United States Government.

#### DISPOSITION INSTRUCTIONS

Destroy this report when it is no longer needed.  
Do not return it to the originator.

REPORT DOCUMENTATION PAGE		READ INSTRUCTIONS BEFORE COMPLETING FORM
1. REPORT NUMBER AVRADCOM TR80-F-9	2. GOVT ACCESSION NO. AD-A094	3. RECIPIENT'S CATALOG NUMBER 756
4. TITLE (and Subtitle) Service Life Determination for the UH-60A (Uttas) Helicopter Elastomeric Bearings		5. TYPE OF REPORT & PERIOD COVERED Final Report Aug 7 1978 to April 1980
7. AUTHOR(s) Ernest P. Gaudette		6. PERFORMING ORG. REPORT NUMBER APE79-021
8. PERFORMING ORGANIZATION NAME AND ADDRESS Lord Kinematics 1635 W. 12th St. Erie, Pa. 16512		9. CONTRACT OR GRANT NUMBER(s) DAAG46-78-C-0038
11. CONTROLLING OFFICE NAME AND ADDRESS Army Aviation Research & Development Command St. Louis, Missouri 63166		10. PROGRAM ELEMENT, PROJECT, TASK AREA & WORK UNIT NUMBERS D/A Proj.: 1757095 AMCMS Code: 1498-94.5 57095 (YYS)
14. MONITORING AGENCY NAME & ADDRESS (if different from Controlling Office) Army Materials & Mechanics Research Center Watertown, MA 02172		12. REPORT DATE April 1980
16. DISTRIBUTION STATEMENT (of this Report) Approved for public release; distribution unlimited (18) USAAVRADCOM, AMMRC (11) TR-80-F-9, TR-84-25		13. NUMBER OF PAGES
17. DISTRIBUTION STATEMENT (of the abstract entered in Block 20, if different from Report)		15. SECURITY CLASS. (of this report) Unclassified
18. SUPPLEMENTARY NOTES AMMRC TR80-25 N.H.		16. DECLASSIFICATION/DOWNGRADING SCHEDULE N/A
19. KEY WORDS (Continue on reverse side if necessary and identify by block number) UH-60A Helicopter      Elastomers      Predictions Helicopters      Bearing      Blackhawk Fatigue      Life Expectancy		
20. ABSTRACT (Continue on reverse side if necessary and identify by block number) A method for predicting the endurance life of the elastomeric bearings on the UTTAS helicopter rotor is presented. The critical layers, based on elastomer strain, are determined analytically for these two bearings. Representative standard laboratory test specimens, bonded with the specified elastomers are subjected to the same static and typical dynamic strains, and tested to failure. Two resulting S-N curves are reported, one for each of the two rotor elastomeric bearings. A short verification of Miner's cumulative damage theory is also conducted and reported.		

407968

JP

## FOREWORD

This project was accomplished as part of the U. S. Army Aviation Research and Development Command Manufacturing Technology program. The primary objective of this program is to develop, on a timely basis, manufacturing processes, techniques, and equipment for use in production of Army Material. Comments are solicited on the potential utilization of the information contained herein as applied to present and/or future production programs. Such comments should be sent to: U. S. Army Aviation Research and Development Command, ATTN: DRSA V-EXT, P.O. Box 209, St. Louis, MO 63166.

The work described in this report was accomplished under a contract let and monitored by the U. S. Army Materials and Mechanics Research Center (DAAG46-78-C-0030).

# TABLE OF CONTENTS

<u>SECTION</u>	<u>Page</u>
LIST OF TABLES	4
LIST OF FIGURES	5
LIST OF PHOTOGRAPHS	6
OBJECTIVE	7
INTRODUCTION	8
Scope	8
Qualifying Assumptions	9
Realism of Load/Motion Conditions	9
Manufacturing Considerations	10
Environmental Considerations	10
Geometry Effects	11
Determination of Critical Layer	11
Failure Definition	12
Validity of the Method	12
Limitations of the Method	12
Data Scatter	13
Low Cycle Fatigue Inputs	13
PREDICTION METHOD	14
Introduction	14
Modelling of Elastomeric Bearings	14
Finite Element	
Analysis	19
Selection of Critical	
Layer	20
(a) Lord P/N LB4-1034-2-1	20
(b) Lord P/N LB5-1034-1-1	20
Metal Shim Fatigue Analysis	20
Critical Elastomer Layer Modeling	21
Test Procedure and Spectrum	27
Test Machines and Data Recording	29
Results of Test	33
Test Result Comments	61
Fatigue Curve Presentation	61
Life Prediction	65
MINER'S CUMULATIVE DAMAGE THEORY TEST	69
SUMMARY OF CONTRACT REQUIREMENTS	
AND WORK PERFORMED	73
CONCLUSIONS	76
RECOMMENDATIONS	79

-3-

Accession For	NTIS GRA&I	<input checked="" type="checkbox"/>	<input type="checkbox"/>	<input type="checkbox"/>
	DTIC TAB	<input type="checkbox"/>	<input type="checkbox"/>	<input type="checkbox"/>
	Unannounced	<input type="checkbox"/>	<input type="checkbox"/>	<input type="checkbox"/>
	Justification	<input type="checkbox"/>	<input type="checkbox"/>	<input type="checkbox"/>
By	Distribution/			
	Availability Codes			
1st	Avail and/or			
	Special			

LIST OF TABLES

<u>Title</u>	<u>Page</u>
1. Common Physical Parameters between the Actual Bearings and Test Specimens	27
2. Test Spectrum	29
3. E-297 Machine Parameters	30
4. Fatigue Test Result Summary	35
5. S-N Curve Equations	62
6. Service Life Prediction	66
7. Comparison of Life Predictions between the Laboratory Test Specimens and the Original Design Analysis	68
8. Miner's Cumulative Damage Theory Test Spectrum	70
9. Miner's Cumulative Damage Theory Test Results	70
10. Summary of Methods to Predict Service Life	76

LIST OF FIGURES

<u>Title</u>	<u>Page</u>
1. Lord P/N LB4-1034-2-1	15
2. LB4-1034-2-1 Deformed Grid	16
3. Lord P/N LB5-1034-1-1	17
4. LB5-1034-1-1 Deformed Grid	18
5. LB4-1-34-2-1 Metal Shim Fatigue, Constant Life Diagram	22
6. LB5-1034-1-1 Metal Shim Fatigue Life Diagram	23
7. TL-367, Elastomeric Laboratory Test Specimen	24
8. LB4-1034-2-1, Test Specimen Finite Element Model	25
9. LB5-1034-1-1, Test Specimen Finite Element Model	26
10. LB4-1034-2-1, Fatigue Test Result, $\pm$ 100% Shear Strain	36
11. LB4-1034-2-1, Critical Layer Fatigue Analysis, Specimen G-7, Plotted Data	37
12. LB4-1034-2-1, Critical Layer Fatigue Analysis, Specimen G-8, Plotted Data	38
13. LB4-1034-2-1, Fatigue Test Result, $\pm$ 60% Shear Strain	39
14. LB4-1034-2-1, Critical Layer Fatigue Analysis, Specimen G-9, Plotted Data	40
15. LB4-1034-2-1, Critical Layer Fatigue Analysis Specimen, G-10, Plotted Data	41
16. LB4-1034-2-1, Fatigue Test Result, $\pm$ 27% Shear Strain (3 sheets)	42
17. LB4-1034-2-1, Critical Layer Fatigue Analysis, Specimen G-11, Plotted Data	45
18. LB4-1034-2-1, Critical Layer Fatigue Analysis, Specimen G-12, Plotted Data	46
19. LB5-1034-1-1, Fatigue Test Result, $\pm$ 110% Shear Strain	47
20. LB5-1034-1-1, Critical Layer Fatigue Analysis, Specimen G-7, Plotted Data	48
21. LB5-1034-1-1, Critical Layer Fatigue Analysis, Specimen G-8, Plotted Data	49
22. LB5-1034-1-1, Fatigue Test Result, $\pm$ 70% Shear Strain	50
23. LB5-1034-1-1, Critical Layer Fatigue Analysis, Specimen G-15, Plotted Data	51
24. LB5-1034-1-1, Critical Layer Fatigue Analysis, Specimen G-16, Plotted Data	52
25. LB5-1034-1-1, Fatigue Test Result, $\pm$ 36% Shear Strain, (3 sheets)	53
26. LB5-1034-1-1, Critical Layer Fatigue Analysis, Specimen G-17, Plotted Data	56
27. LB5-1034-1-1, Critical Layer Fatigue Analysis, Specimen G-18, Plotted Data	57
28. LB4-1034-2-1, Critical Layer S-N Curve	63
29. AB5-1034-1-1, Critical Layer S-N Curve	64

LIST OF PHOTOGRAPHS

<u>Number and Title</u>	<u>Page</u>
15028 Natural Rubber Fatigue (E-297)Test Machine	31
15029 Natural Rubber Fatigue (E-297)Test Machine	32
25976 Typical Failure Appearance of Test Specimen During S-N Curve Testing	58
26082 Test Specimen G-11	59
26083 Test Specimen G-12	59
26084 Test Specimen G-17	60
26176 Miner's Theory Test Specimen, G-2	72
26177 Miner's Theory Test Specimen, G-4	72



### OBJECTIVE

The contract, of which this is the final report, had the objective of developing a method to predict the service life of the Sikorsky Aircraft UTTAS Helicopter elastomeric bearings. The report describes a method for predicting the service life of both the UTTAS spherical and thrust bearings in a manner that will effect cost savings and improve accuracy when compared to previously used methods. The prediction technique involves an analytical evaluation of the bearing to determine the critical elastomer and metal shim layer in terms of stress and strain. These values of stress and strain are compared to laboratory generated S-N data, which for the case of the metal shim is obtained from a source such as MIL-HDBK-5C, and for the elastomer the S-N data is obtained from laboratory test specimens. The test program reported here gives a method for obtaining the specimen S-N data for a bearing critical elastomer layer and relating it to a minimum life for a specific bearing.

## INTRODUCTION

### Scope

The work performed under this contract was to develop an improved service fatigue life prediction technique for the Sikorsky UTTAS Elastomeric Bearings and to predict the service life of the bearings. The two Lord bearings designed for installation into the UTTAS main rotor system are LB4-1034-2-1 and LB5-1034-1-1. In each bearing the most critical elastomer layer, in terms of strain, was determined by finite element analysis and the strains calculated for this layer imposed on a standard Lord Kinematics' test specimen. The indicated edge shear strain determined from the finite element analysis was reproduced on the test specimen by a steady compression load, while the dynamic torsional shear strain applied to the specimen was the variable with which the specific S-N curve for the critical layer was developed. Using the S-N curve and the Sikorsky load-motion spectrum, SES701059, a predicted service life of the bearings can be determined. A test to verify Miner's Cumulative Damage Theory, using two test specimens and a spectrum of conditions selected from SES701059, was also performed. The prediction method is documented so that engineering and technical personnel who are not elastomeric bearing specialists can predict elastomeric bearing service life.

It is our belief that reduction of test cost is the area in which the prediction method will have its greatest impact. Laboratory test specimens and existing test machines have been used to the greatest extent possible to minimize cost. Lord Kinematics feels that the potential for increased accuracy is high. However it must be recognized that many of the factors which influence the comparison of laboratory tests of any type to actual service could not be evaluated within the scope of the test program. Among these factors are the realism of load/motion conditions, environmental effects, type of service exposure, and the influence of manufacturing quality.

The prediction method is directly analogous to the methods utilized to predict service life of a metallic part. That is, the structure is analyzed to determine the peak fatigue stress level; S-N material data and Miner's Cumulative Damage Theory are utilized to predict service life. Increased accuracy is provided in the method prediction by actually testing laboratory specimens to verify the analysis.

#### Qualifying Assumptions

Prior to a detailed discussion of the prediction method, a discussion of the basic problem of predicting elastomeric bearing service lives is presented, along with the assumptions used to maintain the work within the defined scope.

Prediction of elastomeric bearing service life is a complex problem in which many of the influences on service life cannot be defined for the bearing designer. In addition, several factors which influence service fatigue life cannot be considered in a program of the scope defined by the contract. Therefore, assumptions are necessary in developing any method for predicting life.

#### Realism of Load/Motion Conditions

The accuracy of any mathematical analysis is directly influenced by the accuracy of the numerical values used as input. This, of course, assumes that the formulae utilized are accurate and based on sound principles. If the formula used to determine fatigue life is a linear relationship between strain and life, then the "error" in service life prediction will be the same percentage error as that between specified service conditions and actual service conditions. However, if the relationship is not linear, as is the case here, then the "error" may be magnified by the calculation.

It must also be recognized that the type of usage in service can vary and also influence test results. A helicopter used in peace time troop transport could conceivably be a less severe load/motion environment compared to the same helicopter in a combat environment.

Application of the method described herein is based on the assumption that the specified load and motion conditions are truly representative of service conditions.

#### Manufacturing Considerations

Accurate prediction of elastomeric bearing service life is dependent on manufacturing considerations for which additional assumptions and requirements must be stated. The materials and processes utilized in the manufacture of the test samples must be essentially identical to those used for the full size elastomeric bearing. The elastomers and adhesive systems must be identical from test sample to full size bearing. Material fatigue data must be obtained on the elastomers and adhesive system specific to the bearing manufacturer, and such data are not of general use in predicting the fatigue life of bearings from another source.

All test specimens used in this program were fabricated using the same elastomer and metal processes as on the actual bearings. Consistent quality of elastomeric bearings is necessary for accurate service life prediction. The elastomeric bearing in service must be truly representative of that which was analyzed or tested in the laboratory.

#### Environmental Considerations

The test procedure does not include environmental testing, primarily because of the complexity that would result. It has been proven in laboratory testing of Lord Kinematics' bearings using Lord elastomers, adhesives, and processes, that reasonably applied environments typical of helicopter service exposure have a

minimal effect on the service life. This was proven in laboratory tests of Lord P/N LM-726-1 elastomeric pitch change bearing for the Bell Model 540 Rotor and the Lord P/N LM-730-2 centering bearing for the Sikorsky CH53-D Rotor Head. It must be assumed that the environmental exposure in service will be typical of that represented by previous laboratory tests and will not be unrealistically severe.

#### Geometry Effects

The stress or strain on an elastomeric bearing in service can result from a number of different load conditions. As an example, the spherical bearing in the UTTAS Rotor System is subjected to both radial and axial (centrifugal) loading as well as motion in the cocking (flapping and lead-lag) and pitch change directions. In the prediction method it is assumed that the state of stress/strain in the critical layer of the bearing can be duplicated in the laboratory test specimen by the properly selected combination of axial compression load and shear motion. It is the belief of Lord Kinematics that the above assumption is valid. Lord Kinematics feels that elastomeric bearings of all geometries can be analyzed to determine stress/strain conditions which, in turn, can be modeled by simple laboratory test specimens.

#### Determination of Critical Layer

Lord Kinematics utilizes a proprietary blend of natural rubber in elastomeric bearings, which is available in several distinct shear moduli. A particular bearing design may incorporate up to 15 different versions of the same basic elastomer, differing in shear moduli.

In the analysis which determines the critical layer of the elastomeric bearing with respect to stress/strain levels, it is assumed that the fatigue life of various elastomers with different various shear moduli is not a variable. Lord Kinematics believes that this is a valid assumption based on previous experience with Lord elastomers in fatigue.

### Failure Definition

The traditional and primary definition of failure at Lord Kinematics for laboratory tests of both full size elastomeric bearings and laboratory samples has been a specified decrease in shear spring rate in a particular direction. The mode of failure of properly designed and manufactured elastomeric bearings is a gradual "wearing out" in which the elastomer is abraded out of the sections, resulting in a gradual decrease in spring rate. Recent tests have used a 10% to 30% decrease in shear spring rate as a failure criterion, and the resulting life has been viewed as the lower limit where the mean minus three sigma point would fall for metal fatigue curves. This definition of failure when applied to a specimen provides a convenient, easily measured criterion. However, it ignores other failure modes which can occur in service such as shim cracking or loss of stability. It must therefore be assumed that the full size elastomeric bearing has been designed so that the mode of failure will be a gradual loss of spring rate duplicating the mode of failure of the lab specimens. This should be a valid assumption for elastomeric bearings designed by Lord Kinematics.

### Validity of the Method

The prediction method of calculating the service life of an elastomeric bearing is based on sound engineering and scientific principles. In this method, it is assumed that Miner's Cumulative Damage Theory is applicable to the fatigue of elastomer in a manner analogous to metal fatigue. Based on previous experience, Lord Kinematics believe this to be a valid assumption.

### Limitations of the Method

The prediction method is valid for bearings of any configuration provided that the compression loading is essentially steady state in nature. This is true of the Sikorsky UTTAS bearings since the cyclic centrifugal (compression) load is a

small percentage (5-10%) of the normal centrifugal force, and based on Lord Kinematics experience, its effect can be safely ignored. Lord Kinematics considers the theory supporting the prediction method valid for any configuration or mode of loading. However, the number of test samples and the detailed test procedure would of necessity be modified to evaluate the effects of alternating compression. It must be pointed out that the data presented in this report is only valid for the bearings under consideration and cannot be used to predict the life of any other elastomeric bearing. There are a number of parameters inherent in the elastomer, such as base material, blending ingredients, cure system and adhesive, which will influence the prediction results.

#### Data Scatter

It has been assumed that minimal scatter will occur, minimizing the number of data point replications which are necessary. This assumption was made in order to minimize test cost. Lord Kinematics' experience with similar tests, both laboratory specimens and actual elastomeric bearings, indicates that this is a valid assumption.

#### Low Cycle Fatigue (Ground-Air-Ground) Inputs

The prediction method assumes that the primary mode of elastomeric bearing failure in service will be due to high cycle shear fatigue. Failure under low cycle repeated loading due to Ground-Air-Ground (G-A-G) loading, instabilities under maximum load conditions, or other modes of failure are considered beyond the scope of the contract. It is assumed that adequate consideration has been given to these possible failure modes and that an evaluation either empirical or by tests of actual bearings has been made. This is a valid assumption for the Sikorsky UTTAS bearings designed and manufactured by Lord Kinematics.

## PREDICTION METHOD

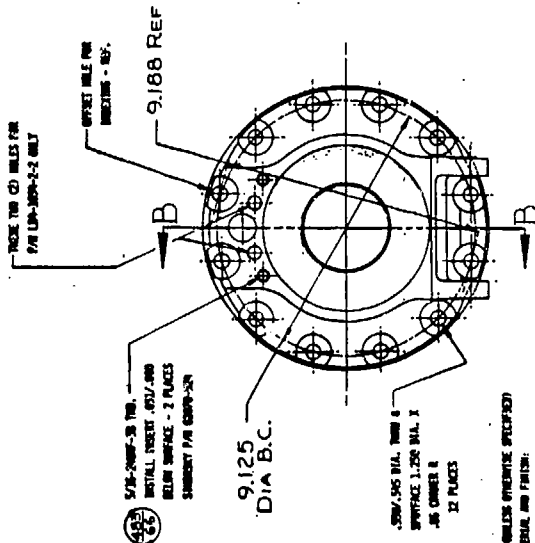
### Introduction

The Lord Kinematics approach to calculating the fatigue life of the Sikorsky UTTAS elastomeric bearings utilizes the same philosophy as metal fatigue analysis. The method is structured to enable engineering and technical personnel who are not specialists with this technology to predict service lives. It will require analytical ability, materials data, and the validity of the assumptions previously stated.

### Modelling of the Elastomeric Bearings

The elastomeric bearings for which a predicted service life is to be obtained was first modeled for a finite element computer analysis. The modeling consisted of defining the bearing geometry as closely as possible and specifying the material properties for the elastomer layers, metal shims, and attachment features. Figures 1 and 2 are the engineering drawing and finite element model respectively of Lord P/N LB4-1034-2-1, while Figures 3 and 4 are the engineering drawing and finite element model respectively of Lord P/N LB5-1034-1-1. The finite element models shown in Figures 2 and 4 are deformed grids; that is, they reflect the behavior of the bearing after imposition of an axial deflection. This deflection in the bearing causes the elastomer layers to bulge and produce a shear strain at the edge of each layer. The deflection in the bearing can be converted to a corresponding load which produced the deflection and the load compared as a ratio to the actual axial load through the bearing. In this manner the actual strains and stresses in the bearing can be evaluated.



[illegible][illegible]

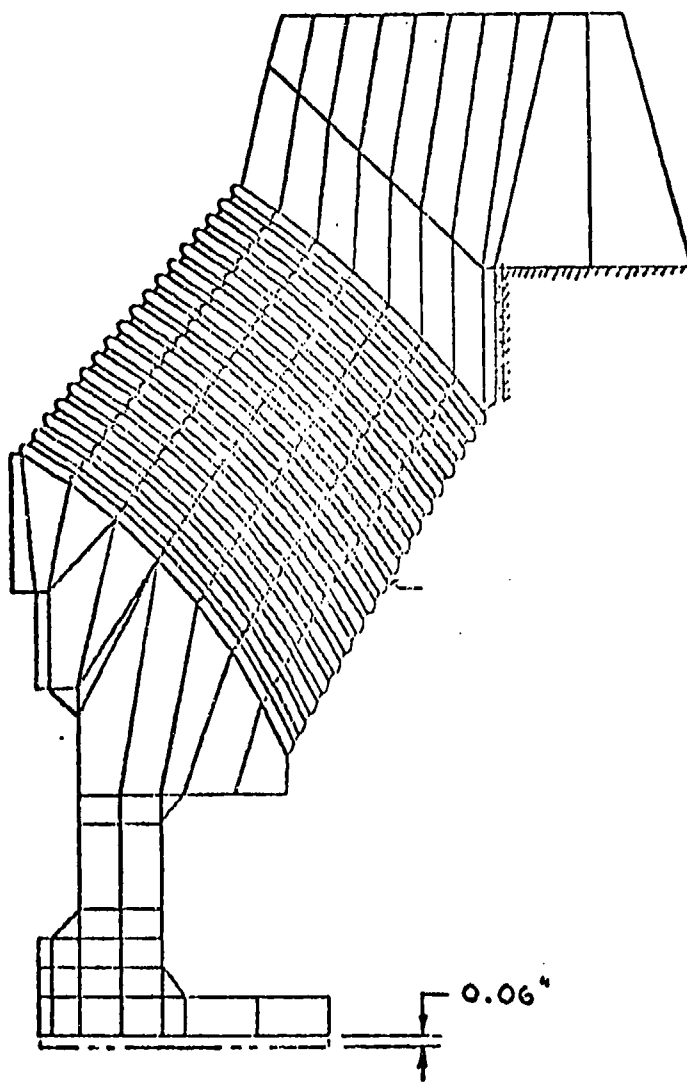
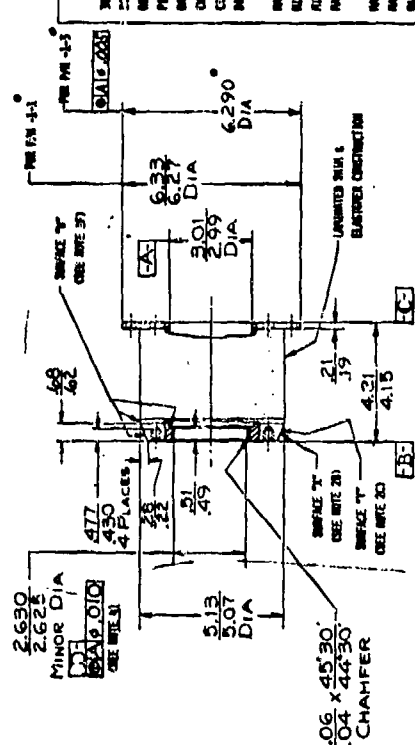
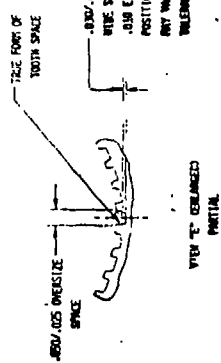


Figure 2. LB4-1034-2-1 Deformed Grid



COND.	PERCENT OCCURRENCE	PITCH STATIC ± VIBRATORY (DEG.)	FREQ. CPM
1	10.3314	9.042 ± 1.014	250
2	7.5594	10.262 ± 3.045	
3	11.2204	6.411 ± 3.8283	
4	21.7905	13.42 ± 6.411	
5	19.2937	7.300 ± 5.465	
6	15.457	13.394 ± 6.96	
7	7.7362	23.55 ± 7.917	
8	8.8075	14.264 ± 7.787	
9	.0035	13.79 ± 9.403	
10	0.0059	14.26 ± 17.576	254

[illegible]

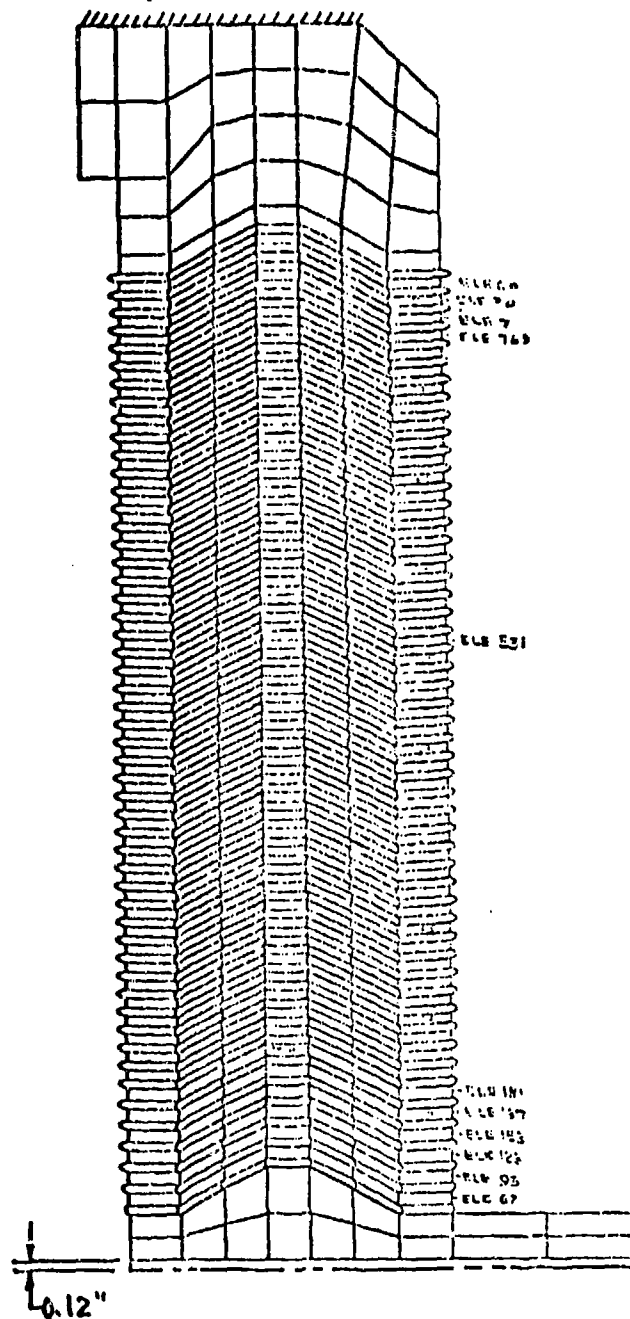
NOTE: GO GAUGE TO BE MADE MIN. EFFECTIVE TOOTH SPACE WIDTH. NO GO GAUGE TO BE MADE TO MAX. DIMENSIONAL TOOTH SPACE WIDTH.  
ABOVE DATA SIZE PLATING OR PROTECTIVE FINISH.

ALL INFORMATION CONTAINED  
HEREIN IS UNCLASSIFIED  
DATE 08-20-2008 BY 60322  
UCBAW

[illegible]

115-3074-1-3	70286-307002-046	REV. 77
115-3074-1-1	70286-307002-046	REV. 77
1150 P/A	STEWART P/A	REV. LETTER

[illegible]



DEFORMED GRID

Figure 4. LORO LBS-1034-1-1 WITH AXIAL LOAD

The axial load through both UTTAS bearings is a result of the centrifugal blade loading in the helicopter. This load is assumed to be steady, as mentioned in the introduction, and the edge shear strain which this steady load produces will be reproduced on the test specimen.

#### Finite Element Analysis

A Lord computer program entitled "SARLAS" was utilized to perform the finite element analysis of the subject bearings. This computer program is a derivative of the program "TEXGAP" which was developed at the University of Texas by Professors E. B. Becker and R. S. Dunham. The computer program "TEXGAP" is not available from Lord Kinematics. It is distributed and is available only from Professor E. B. Becker at the University of Texas. The program was financed by the U. S. Air Force through United Technology. These programs are capable of analyzing a complex structure of metals, composites, and rubber-like materials without the simplifying assumptions of rigid metals (shims) or simple and regular geometries as in the closed form solutions. The unique characteristic of these programs is the ability to analyze materials with a shear modulus many orders of magnitude less than the bulk modulus. This is commonly spoken of in terms of "incompressible" or nearly incompressible materials (Poisson's Ratio = 0.499995). The computer program "SARLAS" is proprietary to Lord Kinematics and consists of "TEXGAP" with revisions to input and output format to facilitate usage and interpretation of results.

In summary, "TEXGAP" was used to determine the level of strain in each elastomer layer. The critical layer was then determined in terms of direct and indirect shear strain. "TEXGAP" was also used to determine the level of stress in each metallic shim, and using available metal S-N data (i.e., MIL-HDBK-5) a fatigue analysis of the shim was performed.

#### Selection of Critical Layer

A. Lord P/N LB4-1034-2-1

The critical layer in terms of elastomeric edge shear strain was selected using the "SARLAS" analysis. The highest calculated value occurred in the 17th layer from the spherical center at the inside diameter.

B. Lord P/N LB5-1034-1-1

The critical layer of this bearing in terms of elastomeric edge shear strain was also selected using the "SARLAS" analysis. The highest calculated value occurred in the 1st layer from the small end plate at the outside diameter.

#### Metal Shim Fatigue Analysis

The metal shim fatigue analysis was performed on the bearings for Sikorsky.

The analytical approach employed in the shim stress analysis utilized a combination of finite element analysis, strain gage data and parametric analysis. The bearings were analyzed using SARLAS in the axial loading mode.

A listing of the maximum and minimum stresses and strains (by material) and their locations in the bearings was obtained. The shims where the maximum hoop stress and the maximum combined stress were reported were then used for the detailed analysis and comparison with available data. The change in hoop stress, due to a flap (cocking) input to a spherical thrust bearing is linear and is affected mainly by axial loading while cocking. A parametric analysis utilizing strain gage data from previous testing of similar bearings in conjunction with the SARLAS analysis was used to obtain the predicted level of alternating stress with cocking angle.

The fatigue life of the thrust bearing shims is dependent primarily on the Ground-Air-Ground axial loading with little or no change due to the torsional (pitch) input. Strain gage analysis of similar thrust bearings indicate an acceptable level of correlation with SARLAS finite element analysis; therefore, the calculated SARLAS value was used.

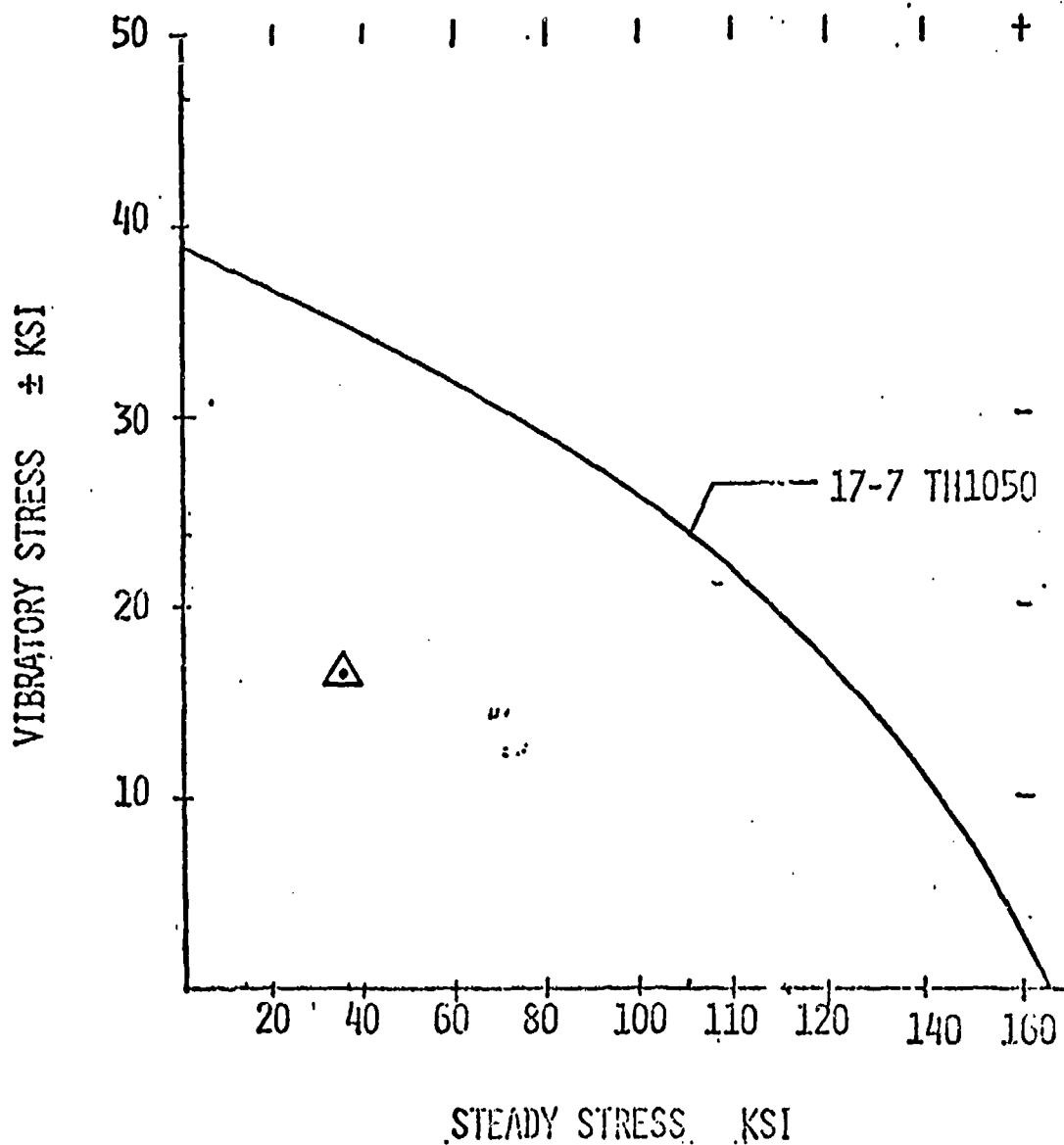
The results of the spherical shim analysis are presented on a Working Stress Diagram for  $10^8$  cycles derived from Sikorsky data, to demonstrate shim life acceptability (Figure 5). The results of the thrust shim analysis is presented on a mean  $-3\sigma$ -N curve to demonstrate shim life acceptability (Figure 6), also derived from Sikorsky data.

#### Critical Elastomer Layer Modeling

The laboratory test specimen selected was a bonded right circular cylinder ("disk") configuration. Figure 7 is a drawing of the specimen, TL-367-1-4, as used in the test. The bonded specimens had the identical elastomer and adhesive system as the critical layer in the respective bearings. A finite element analysis was conducted on the laboratory test specimen for each of the two critical layer elastomers. A deflection of .005 inch was imposed on the test specimen model which was then translated into an equivalent load and in an induced edge shear strain. The calculated edge shear strain was scaled to give the required loading necessary to produce the critical edge shear strain on the test specimen. Figures 8 and 9 are computer drawings of the deformed shape of the test specimen. It was only necessary to model one quarter of the test specimen to obtain the required information, due to its symmetrical shape. Table 1 presents the common physical parameters between the actual bearings and their respective test specimens.

# CONSTANT LIFE DIAGRAM(1)

WORKING STRESS LEVELS AMMRC Contract DAAG46-78-C0030  
Final Report APE79-021  
10<sup>8</sup> CYCLES



(B)

Figure 5. LB4-1034-2-7 Metal Shim  
Fatigue Constant Life Diagram



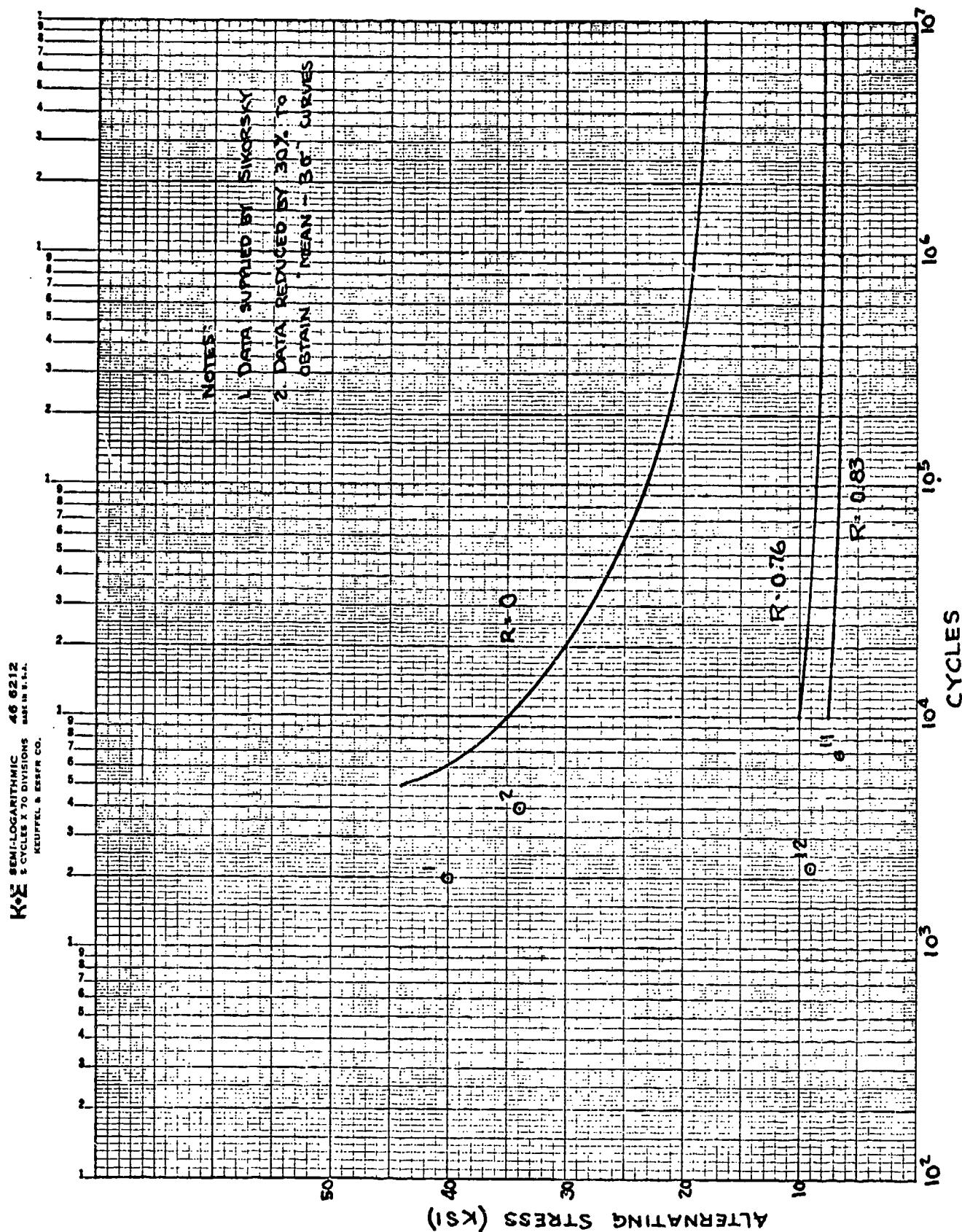
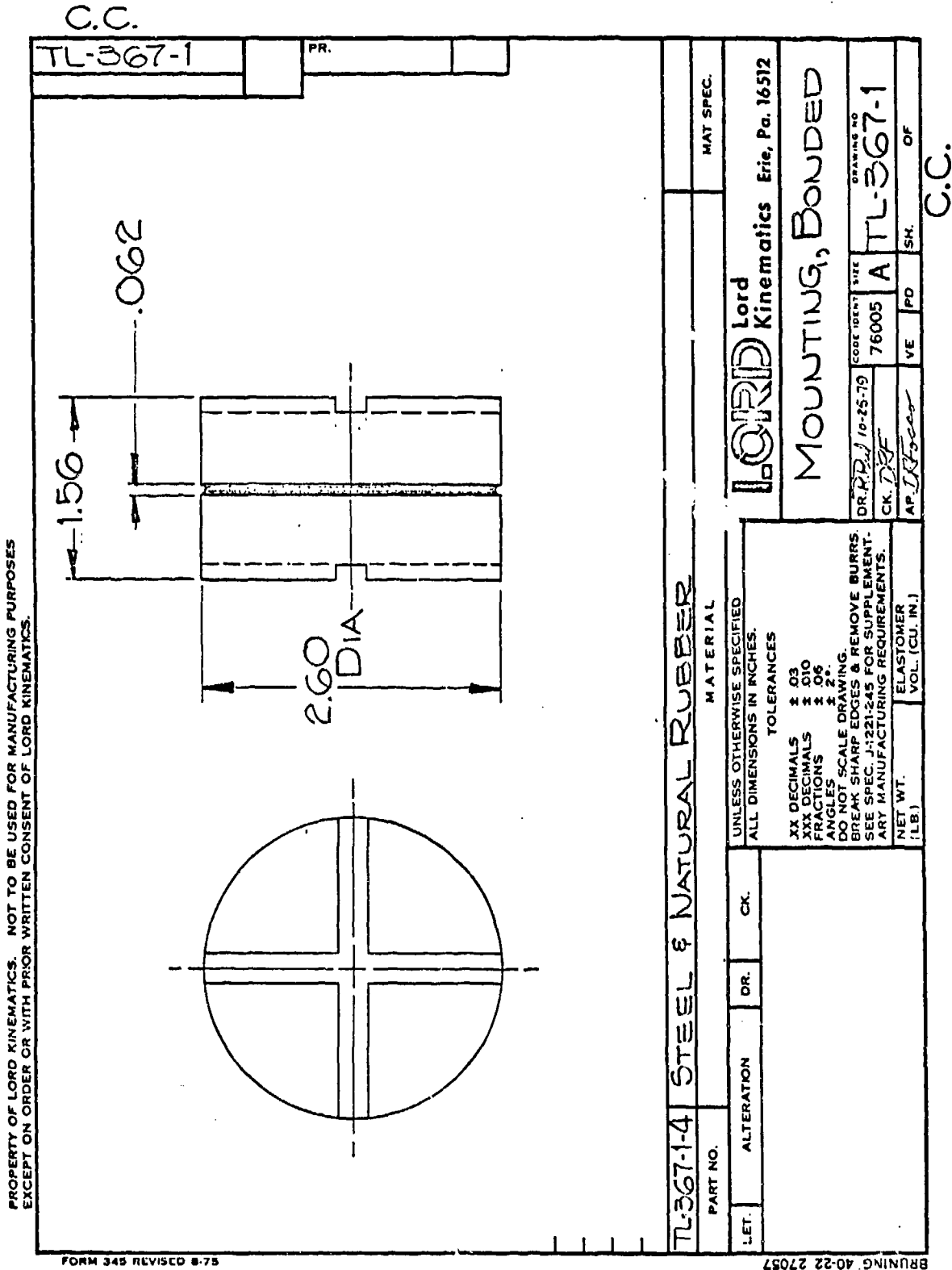


Figure 6 LB5-1035-1-1 Metal Shim Fatigue Life Diagram

Figure 7 TL-367, Elastomeric Laboratory  
Test Specimen



41	42	43	44	45	46	47	48	49	50
31	32	33	34	35	36	37	38	39	40
21	22	23	24	25	26	27	28	29	30
11	12	13	14	15	16	17	18	19	20
1	2	3	4	5	6	7	8	9	10

# DEFORMED GRID

AMRC SERVICE LIFE DET CRI LAY MODEL EPG 9/05/78 X833-G AXIAL=.005 TORS.=1 DEG

Figure 8 LB4-1034-2-1, Test Specimen Finite Element Model

ARLAS

ATE 09/05/78

TIME 08 30 311

41	42	43	44	45	46	47	48	49	50
31	32	33	34	35	36	37	38	39	40
21	22	23	24	25	26	27	28	29	30
11	12	13	14	15	16	17	18	19	20
1	2	3	4	5	6	7	8	9	10

-26-

## DEFORMED GRID

4MRC SERVICE LIFE DET CRI LAY MODEL EPG 9/05/78 X833-G AXIAL=.005 TORS.=1 DEG

IRLAS

Figure 9 LB5-1034-1-1, Test Specimen Finite Element Model

ITE 09/05/78

00 00 00

TABLE 1

Common Physical Parameters Between the Actual Bearings  
and Test Specimens

<u>Item</u>	<u>LB4-1034-2-1</u>	<u>LB5-1034-1-1</u>
Critical Layer	17 <sup>a</sup>	1 <sup>b</sup>
Elastomer	MAD008	MAD013
Modulus	125 psi	215 psi
Test Specimen Com- pressive Load	18345 lbs.	23535 lbs.

<sup>a</sup> Layers numbered from spherical focal point

<sup>b</sup> Layers numbered from small end plate

Test Procedure and Spectrum

The laboratory specimens were tested in pairs for each point on the S-N curve. The test was conducted under an applied static axial load which produced the same edge shear strain as in the bearing when operated as specified in SES701059. The actual compression load used with each bearing test was presented in Table 1 above. An oscillating torsional input (direct shear strain) was imposed on each pair of test specimens with a total of three pairs of specimens and three different oscillating torsional inputs used to generate the S-N curve. After every 10,000 cycles of input, the static torsional stiffness of each specimen was measured under zero (nominal) applied static axial load. The initial measurement, taken at 1000 cycles, was used as a reference. A data point was permanently recorded when the torsional stiffness changed by 5% or the cycles had doubled since the last recorded data point. When the measured stiffness changed by more than 20% of the reference value, the sample was considered failed, and the number of cycles to reach this point was

taken as the fatigue life of the specimen. The average of the two specimen values at each input condition was taken as the fatigue life to be used in constructing the S-N curve. The above test sequence was conducted two times--once for each of the two Sikorsky UTTAS bearings. It should be noted that during the long term testing three test specimens did not reach the failure criterion of a loss of 20% shear stiffness. The reasons for removal are discussed later in the Test Results section of this report.

The oscillating torsional inputs were selected to give a range broad enough to encompass the shear strains encountered by the bearing, yet provide for a reasonable test time. The actual oscillating torsional angle for each specimen was calculated using Equation 1 below:

$$\theta = \frac{t E_s (57.296)}{r (100)} \quad (1)$$

where:

- $\theta$  = Torsional angle in degrees
- $t$  = Specimen elastomer thickness
- $r$  = Specimen elastomer radius
- $E_s$  = Required direct shear strain in %

The test spectrum is presented in Table 2.

TABLE 2

Test Spectrum

<u>Bearing P/N</u>	<u>Elastomer</u>	<u>Direct Shear Strain</u>	<u>Test Specimen Torsional Angle</u>
LB4-1034-2-1	MAD008	+ 100%	2.84°
		+ 60%	1.71°
		+ 27%	0.77°
LB5-1034-1-1	MAD013	+ 110%	3.13°
		+ 70%	2.00°
		+ 36%	1.02°

Test Machines and Data Recording

Lord Kinematics believes that commercially available test machines could have been utilized to perform the testing. However, an existing Lord designed machine was selected to minimize cost. The Lord designation for the test machine is E-297.

The E-297 test machine subjects a thin layer of elastomer to a combination of torsional deflection and compressive force about an axis normal to the layer. Test samples consist of elastomer bonded between plane-sided metal discs. Lord P/N TL367, the sample normally employed, has a diameter of 2.5 inches. Existing configurations and tooling were used to fabricate the samples and to model the strain conditions required.

Each of the two machines available has two test stations. Each station consists of a central rotary hydraulic actuator, with a test sample at each end of its shaft, strain gaged transducers sensitive to both torque and axial force, and a linear hydraulic force actuator at each end. Two samples can be accommodated in each test line, four per machine, giving a total of eight. Control is by closed-loop servohydraulics. Three loops are employed, one for torsional motion, and one for each of the two

axial force actuators. Photographs numbers 15028 and 15029 show the test machine as configured for the test. The performance parameters are given in Table 3. The Lebow Model #6468 thrust-torque sensor and the Brush Metrisite #31 38 10 RVDT were both calibrated prior to starting the test to National Bureau of Standards requirements.

Motion data was taken from the Gilmore 1060 signal conditioners used to handle the feedback signals in the servo loops. Force data was sensed by Lebow type 6468 thrust-torque sensors, connected to Gilmore Model 1050 signal conditioners.

TABLE 3

E-297 Machine Parameters

SUMMARY OF CAPABILITIES:

Maximum Compression Load	80,000 lbs.
Compression Cylinder Stroke	+ 1 inch
Maximum Torque	21,700 lb-in
Maximum Torsional Angle	100 + 5°
Opening Size	2 x 13 x 13 inches
Number of Test Stations	4 (with 2 test samples per station)
Instrumentation	Lebow Model #6468 Thrust-Torque Sensor (Fatigue Ratings: 25000 lb-in torque, 75000 lb thrust)

LOCATION

Lord Kinematics High Energy Test Lab

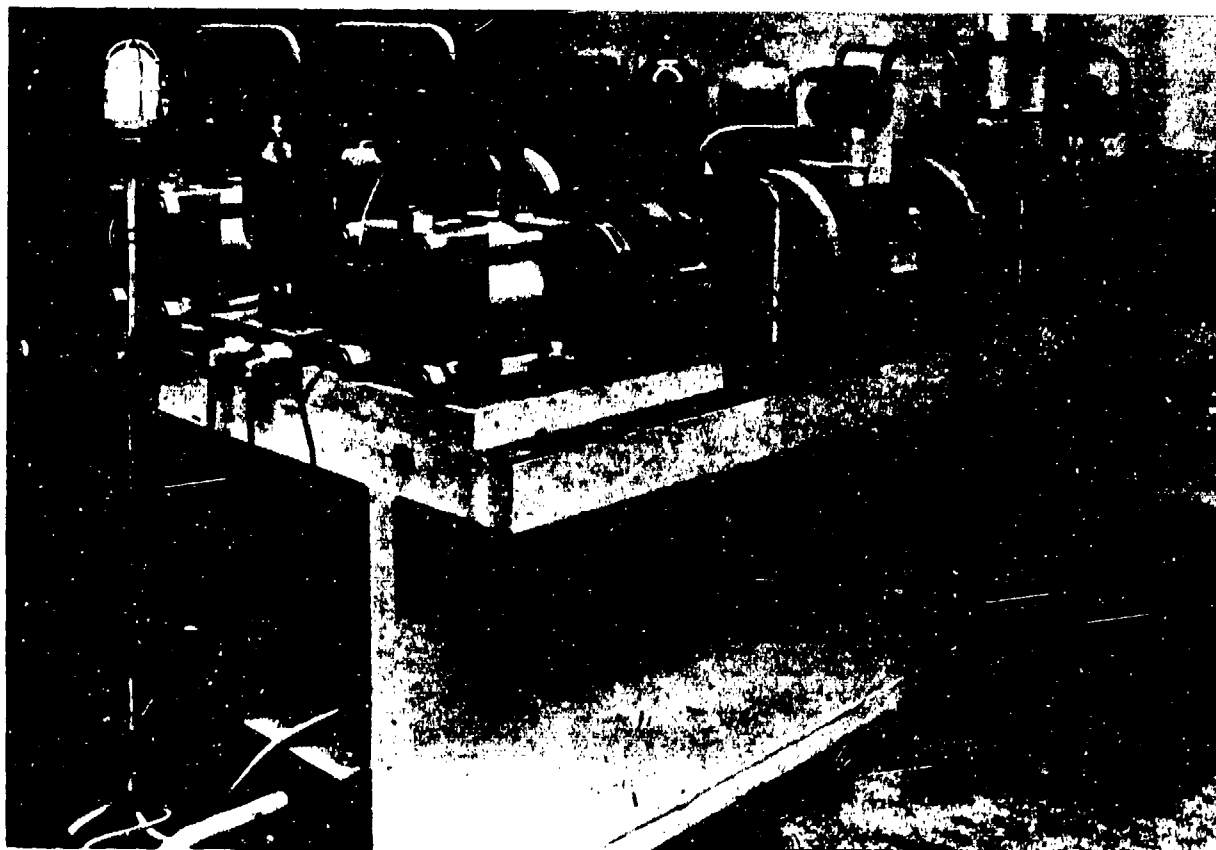
FUNCTION

This machine is designed to apply torsion and compression loads to thin rubber discs. It can apply various combinations of static and dynamic torsion or compression.

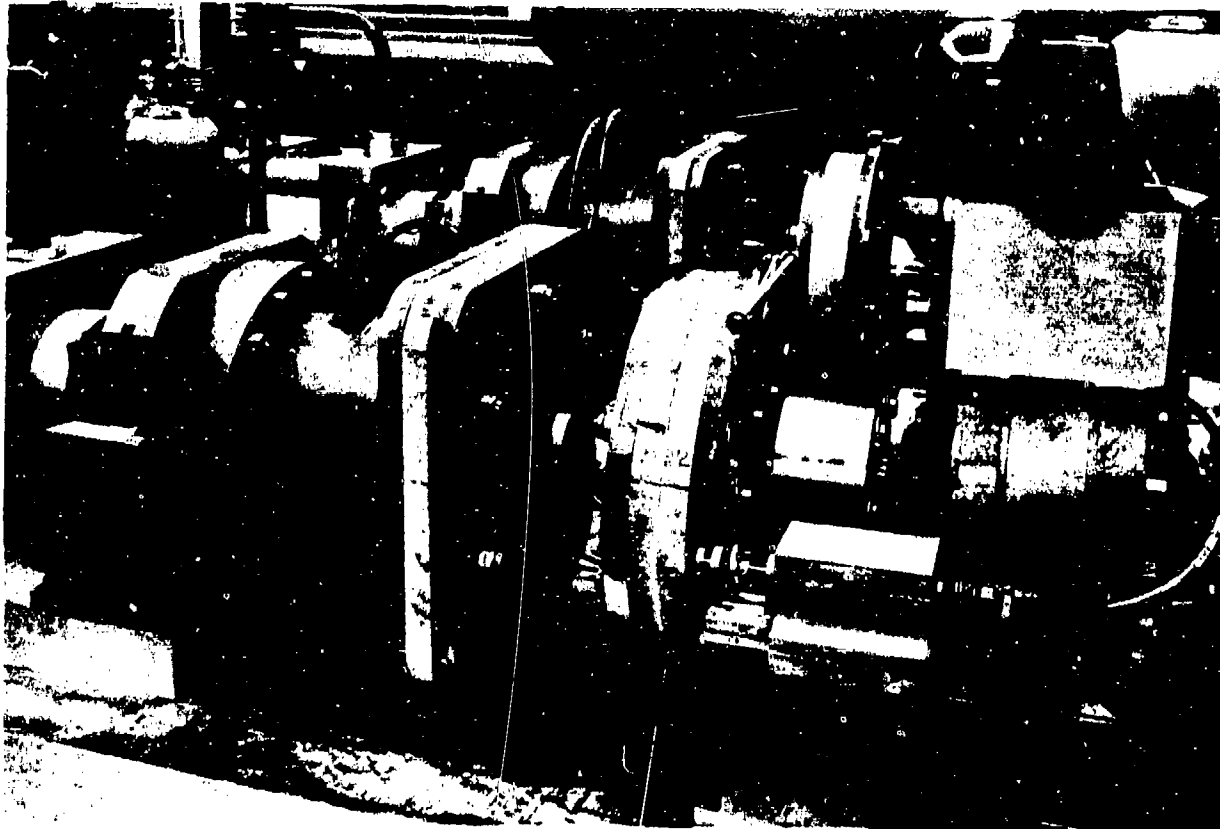
STANDARD TEST SPECIMEN

TL-367-1





Photograph 15028  
NATURAL RUBBER FATIGUE (E-297) TEST MACHINE



Photograph 15029  
NATURAL RUBBER FATIGUE (E-297) TEST MACHINE

Data from the signal conditioners is acquired by multiplexing into a Hewlett-Packard Model 9600E digital computer system. Both force and motion signals are subjected to Fourier analysis and the fundamental components of their waveforms are used to determine the torsional spring rate.

### Results of Test

A frequency verification test was performed to determine the highest of three selected frequencies which did not produce results which differed significantly from the 4.3 Hz results. The 4.3 Hz frequency is equivalent to the operating frequency of the Sikorsky UTTAS main rotor. The test frequencies selected were 10 Hz, 7 Hz and 4.3 Hz. A total of six specimens were tested in three pairs at the most severe input condition and stiffest elastomer stock. The initial test was conducted at 10 Hz with the specimens failing at an average of 975,000 cycles. The control test was run at 4.3 Hz with these specimens failing at an average of 1,270,000 cycles. The indicated spring rate data for the 10 Hz test was erratic when compared to the 4.3 Hz test data. The test machine at 10 Hz required frequent adjusting and tuning, which occasionally required the machine to be shut down, thus indicating that the test machine was strained beyond its capability. These two reasons prompted a third test at 7 Hz.

The two specimens tested at 7 Hz failed at an average of 1,389,000 cycles. This is within 9.3% of the cycles to failure at 4.3 Hz, as compared to 30.3% for the 10 Hz test. There was also no unscheduled stoppage of the test machine. Based on this test a determination was made to conduct the remainder of the test at 7 Hz.

The specimen fatigue test was conducted as described in the Test Procedure section of this report. A total of six test specimens, two at each of three conditions, were tested to develop the S-N curve for the critical layer of each bearing. The data was tabulated in terms of torsional shear spring rate and the number of fatigue cycles

which transpired to effect that spring rate. This tabulated data was then plotted for each specimen as torsional shear spring rate versus cycles to failure. As mentioned earlier, the assumed failure criterion is a 20% loss of shear spring rate when compared to a reference spring rate taken at 1000 cycles. The final method of data presentation is the construction of the actual S-N curve developed from the direct shear strain in percent at which the specimen was tested versus the average cycles to failure between the two specimens tested at that condition. Table 4 is a comprehensive summary of the test results, listing for each bearing the direct shear strain in percent, the cycles to failure of each test specimen, the average cycles to failure and the figure number where the tabulated and plotted data can be found.

It should be noted once again that three of the four test specimens in the least severe test (27% and 36% direct shear strain) did not fail at the assumed failure criteria. The test was terminated because of severe elastomer abrasion and reversion. Photographs numbers 26082, 26083, and 26084 show the individual test specimen condition at the time of termination.

**TABLE 4**  
**Fatigue Test Result Summary**

**A. Bearing P/N LB4-1034-2-1**

Location of Test Specimen on Machine	Test Specimen S/N	Elastomer	Direct Shear Strain	Cycles to Failure	Average Cycles for S-N Curve	Figure Numbers Tabulated Data	Figure Numbers Plotted Data
West	G-7	MAD008	+ 100%	1749700	1765250	10	11
East	G-8	MAD008	+ 100%	1780800		10	12
West	G-9	MAD008	+ 60%	16744900	14303000	13	14
East	G-10	MAD008	+ 60%	11861100		13	15
West	G-11	MAD008	+ 27%	42760161	42760161	16 (3 shts)	17
East	G-12	MAD008	+ 27%	42760161		16 (3 shts)	18

**B. Bearing P/N LB5-1034-1-1**

Location of Test Specimen on Machine	Test Specimen S/N	Elastomer	Direct Shear Strain	Cycles to Failure	Average Cycles for S-N Curve	Figure Numbers Tabulated Data	Figure Numbers Plotted Data
West	G-7	MAD013	+ 110%	700306	817100	21	22
East	G-8	MAD013	+ 110%	933900		19	21
West	G-15	MAD013	+ 70%	3527600	4490400	22	23
East	G-16	MAD013	+ 70%	5453200		22	24
West	G-17	MAD013	+ 36%	42863045	38330027	25 (3 shts)	26
East	G-18	MAD013	+ 36%	33797000		25 (3 shts)	27

STATION # 2  
PART# TL367-1-5

INPUT CONDITIONS- TORSION: .00+- 2.84  
COMPRESSION: 18340. +-

	WEST		EAST	
SAMPLE #:	G- 7		G- 8	
STATUS:	OFF		OFF	
TEST STARTED:	9:20	1 NOV 78	9:20	1 NOV 78
LAST READING:	9:48	4 NOV 78	11:08	4 NOV 78
	(LB-IN/DEG)	(#CYCLES)	(LB-IN/DEG)	(#CYCLES)
REFERENCE:	139.0	0	142.0	0
	131.8	1 000	132.0	1 000
	131.5	2 000	131.9	2 000
	130.5	4 000	131.5	4 000
	129.8	8 000	130.4	8 000
	130.0	25 300	130.8	25 300
	129.0	55 300	130.8	55 300
	127.7	115 300	129.4	115 300
	129.4	237 500	130.8	237 500
	129.6	477 500	131.7	477 500
	122.2	598 300	119.5	588 300
	135.9	599 200	126.2	599 200
	128.2	609 200	134.7	659 500
	120.3	1 189 500	127.5	709 500
	113.7	1 539 700	120.5	1 399 700
	106.8	1 709 700	113.6	1 609 700
			106.9	1 749 700
	105.2	1 749 700		
			104.8	1 780 800

Figure 10, LB4-1034-2-1  
Fatigue Test Result  
±100% Shear Strain

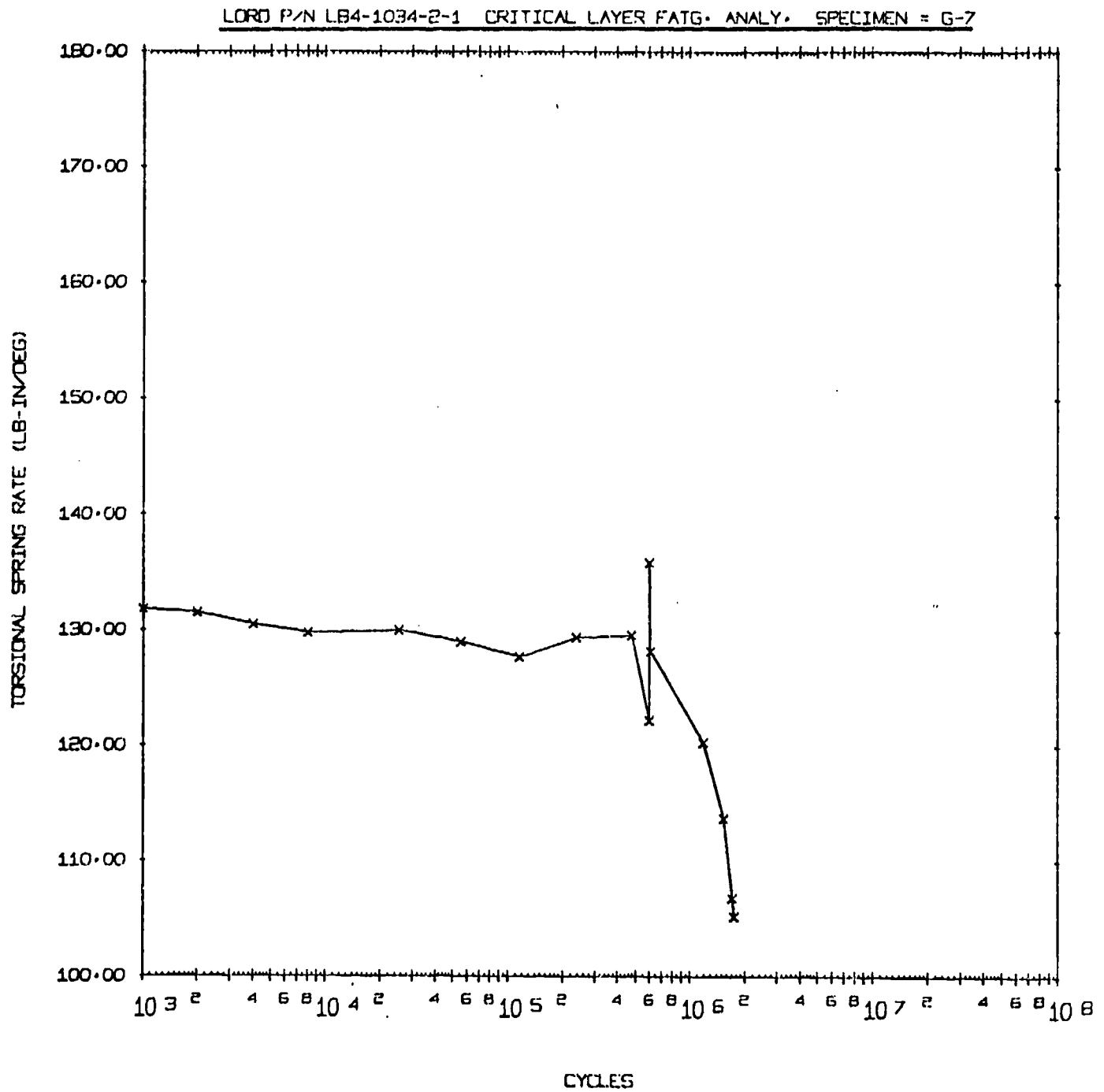


Figure 11

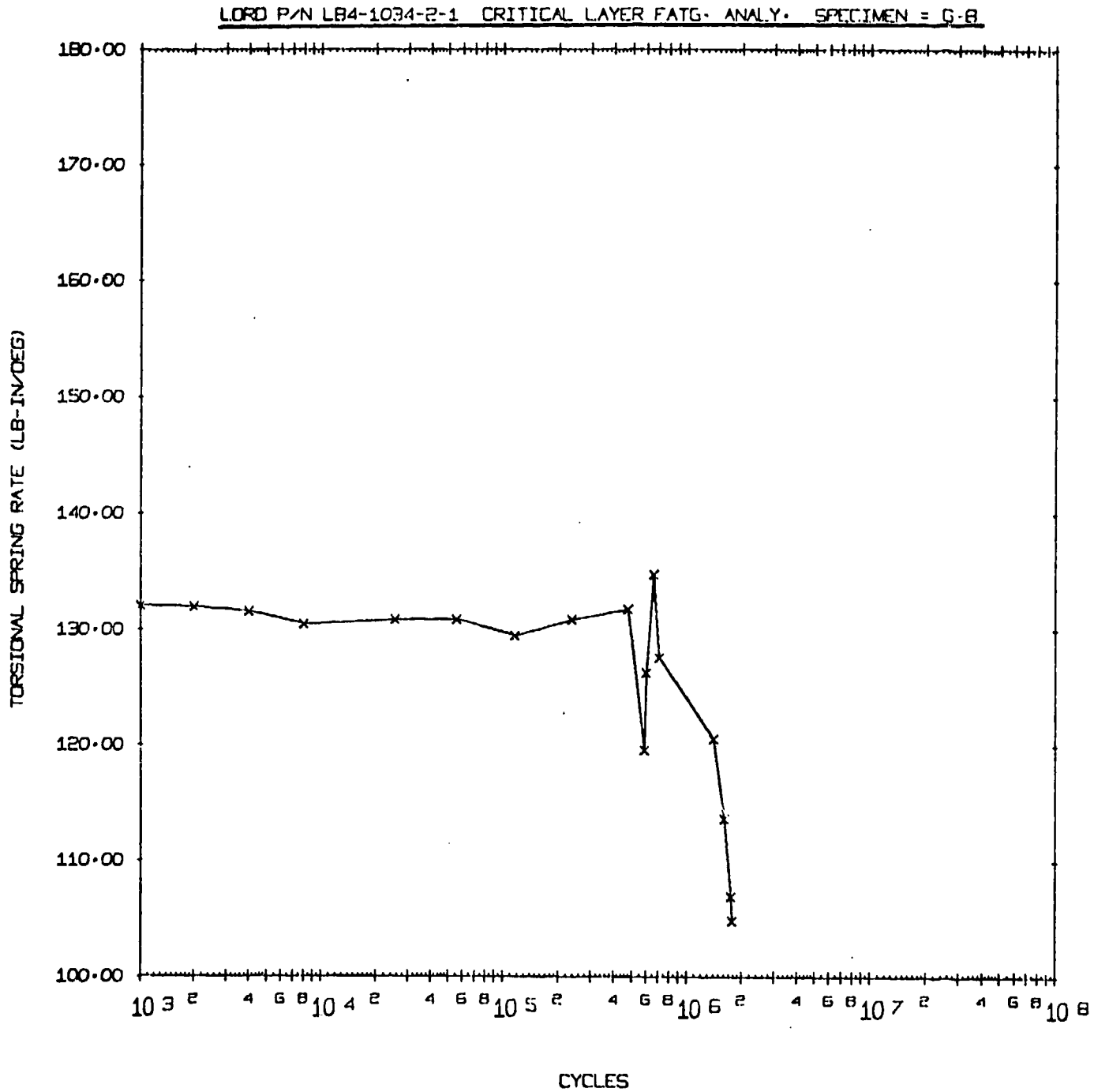


Figure 12



STATION # 2  
PART# TL367-1-5

INPUT CONDITIONS- TORSION: .00+- 1.71  
COMPRESSION: 18340.+-

	WEST		EAST
SAMPLE #:	G- 9		G- 10
STATUS:	OFF		OFF
TEST STARTED:	11:01 22 FEB 79		11:01 22 FEB 79
LAST READING:	13:11 25 MAR 79		16:13 18 MAR 79
	(LB-IN/DEG) (#CYCLES)		(LB-IN/DEG) (#CYCLES)
REFERENCE:	148.6 500		138.0 500
	140.5 1 500		134.8 1 500
	139.6 3 500		134.2 3 500
	138.4 7 500		133.6 7 500
	137.3 15 600		133.0 15 600
	137.1 37 900		133.5 37 900
	137.2 77 900		134.1 77 900
	135.9 188 400		133.1 188 400
	135.5 377 300		133.9 377 300
	148.0 750 600		141.3 750 600
	137.4 760 600		134.4 780 600
	135.5 1 530 700		136.4 1 570 700
	134.3 3 067 300		119.1 3 138 900
	141.7 4 549 300		134.3 3 218 700
	133.6 4 649 400		127.0 3 889 200
	141.0 5 407 100		134.1 3 919 300
	133.2 5 457 100		126.5 5 407 100
	140.6 5 707 600		141.8 5 427 100
	132.8 5 827 600		131.9 5 437 100
	140.5 8 292 000		141.8 5 497 100
	133.3 8 552 000		132.7 5 507 100
	142.3 11 861 100		125.8 7 527 600
	132.1 11 871 100		118.7 9 752 000
	124.9 13 009 700		111.9 11 001 100
	110.5 13 147 500		
	132.0 13 147 500		107.8 11 861 100
	111.9 16 744 900		

Figure 12 LB4-1034-2-1  
Fatigue Test Result  
± 60% Shear Strain

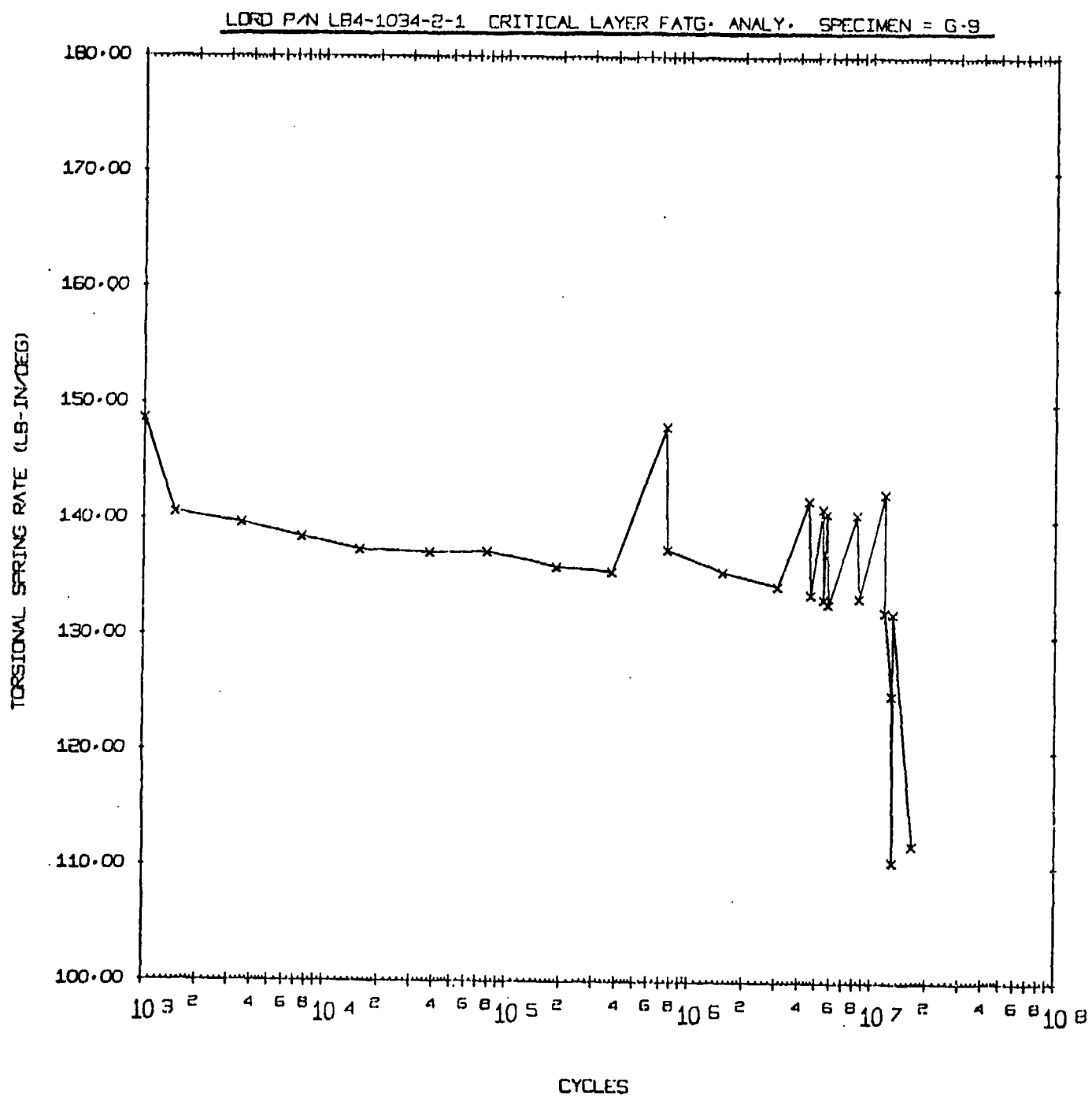


Figure 14

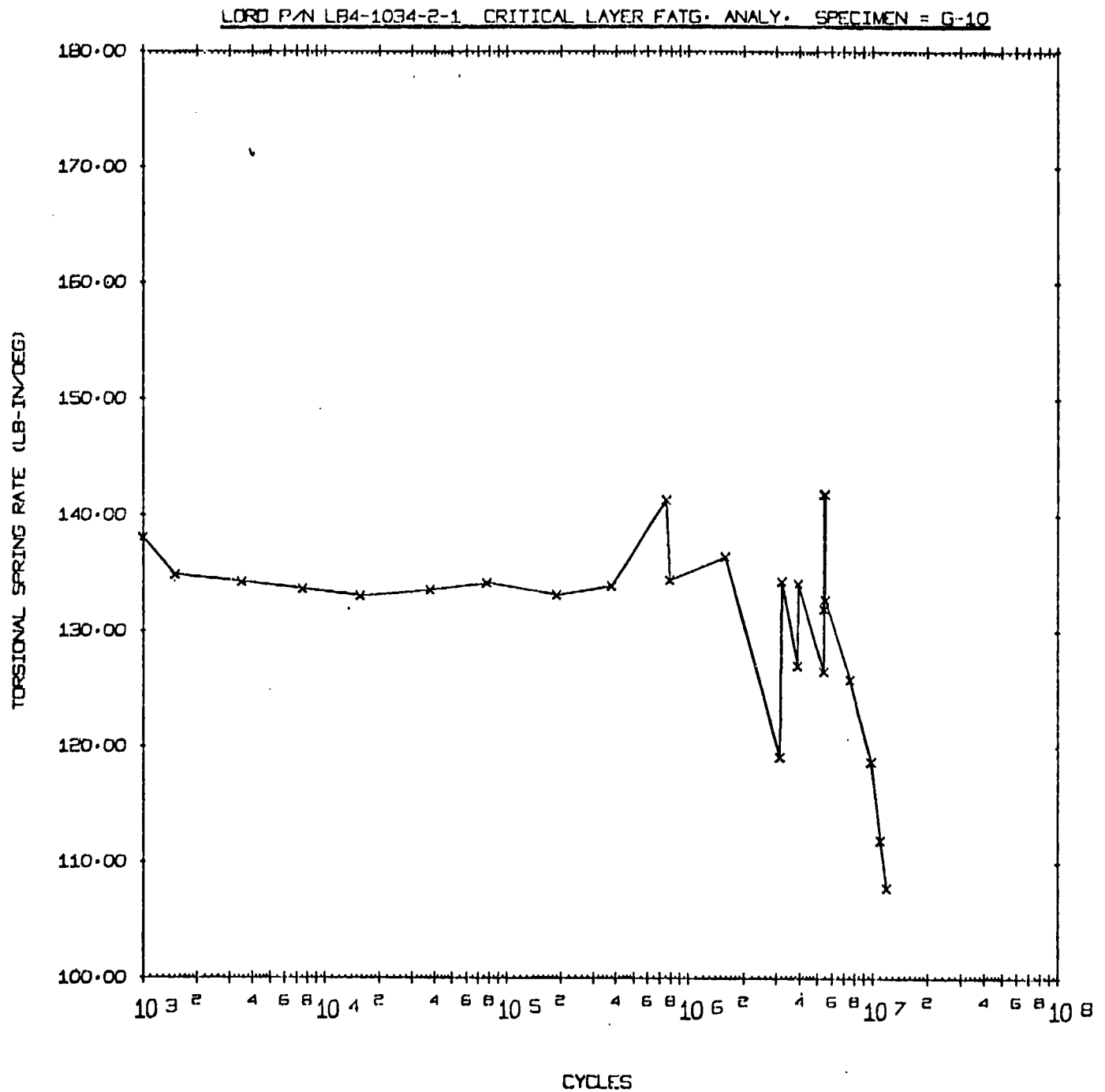


Figure 15

STATION # 1  
PART# TL367-1-5

INPUT CONDITIONS- TORSION: .00+- 77  
COMPRESSION: 18340. +-

SAMPLE #: WEST 1st FILE EAST  
G- 11 G- 12  
STATUS: HOLD HOLD

TEST STARTED: 10:57 16 JUN 79 10:57 16 JUN 79  
LAST READING: 16:15 27 JUL 79 16:15 27 JUL 79

	(LB-IN/DEG)	(#CYCLES)		(LB-IN/DEG)	(#CYCLES)
REFERENCE:	145.9	0		130.4	0
	138.0	1 000		126.1	1 000
	136.6	2 000		125.0	2 000
	136.9	4 000		124.3	4 000
	135.8	8 000		124.4	8 000
	135.4	20 000		124.3	20 000
	134.9	40 000		123.7	40 000
	134.7	82 400		125.7	82 400
	134.9	172 400		128.0	172 400
	135.0	352 400		127.6	352 400
	137.2	720 897		120.1	720 897
	135.8	1 450 997		121.6	1 450 997
	137.1	2 910 197		132.8	1 816 497
	138.3	5 824 297		121.9	2 420 197
	147.7	11 853 609		128.8	2 460 197
	140.4	11 894 609		121.8	3 270 497
				120.4	3 780 497
	140.8	15 085 309		131.8	7 564 597
				121.0	8 134 797
				130.7	8 164 897
				122.4	10 697 497
				133.8	11 853 609
				124.3	11 854 609
				131.6	11 874 609
				117.9	14 619 709
				124.8	14 639 709
				123.0	15 085 309

Figure 16 LB4-1034-2-1  
Fatigue Test Result -  $\pm 27\%$  Shear Strain

\*\* BOOT-UP \*\*\*\*\* SET TIME!!!

STATION # 1  
PART# TL357-1-5

INPUT CONDITIONS-- TORSION: .00+- .77  
COMPRESSION: 18340.+-

SAMPLE #: WEST 2ND FILE EAST  
STATUS: G- 11 G- 12  
HOLD HOLD

TEST STARTED: 10:14 30 JUL 79 10:14 30 JUL 79  
LAST READING: 10:21 4 SEP 79 10:21 4 SEP 79

	(LB-IN/DEG)	(#CYCLES)		(LB-IN/DEG)	(#CYCLES)
REFERENCE:	144.2	0		136.0	0
	142.1	10 000		136.5	10 000
	141.6	30 100		136.6	30 100
	140.5	70 100		134.9	70 100
	140.1	144 000		130.2	144 000
	139.2	294 000		134.2	294 000
	139.1	594 000		135.4	594 000
	141.8	1 194 000		137.3	1 194 000
	139.0	2 388 100		128.2	2 148 100
	139.7	4 780 000		135.3	2 808 100
	138.6	9 568 600		127.3	3 458 100
	129.2	16 612 000		120.3	4 500 000
	138.6	18 711 700		131.4	4 510 000
				118.2	8 022 800
	138.6	18 712 100		130.3	8 322 800
				114.6	8 918 600
				124.1	8 928 600
				116.6	10 748 700
				127.8	10 858 700
				119.4	12 338 700
				112.2	12 498 700
				127.4	12 518 700
				118.6	13 968 700
				125.5	14 148 700
				117.6	15 008 700
				125.6	15 058 700
				129.6	18 712 100

Figure 16. LB4-1034-2-1  
Fatigue Test Result-±27% Shear Strain

(Sheet 2 Of 3)

STATION # 1  
PART# TL367-1-5

INPUT CONDITIONS- TORSION: .00+- .77  
COMPRESSION: 18340. +-

SAMPLE #: WEST 3RD FILE EAST  
STATUS: G- 11 HOLD G- 12 HOLD

TEST STARTED: 10:25 4 SEP 79 10:25 4 SEP 79  
LAST READING: 11:22 24 SEP 79 11:22 24 SEP 79

	(LB-IN/DEG)	(#CYCLES)		(LB-IN/DEG)	(#CYCLES)
REFERENCE:	131.8	0		124.2	0
	131.2	10 000		123.9	10 000
	131.4	20 000		123.5	20 000
	130.7	40 000		123.2	40 000
	130.8	80 000		123.0	80 000
	130.5	160 000		122.3	160 000
	131.2	320 000		122.1	320 000
	139.7	536 900		121.5	646 900
	132.8	716 900		121.3	1 295 000
	135.1	1 440 100		121.2	2 590 900
	134.0	2 880 900		130.1	3 203 500
	142.9	5 885 100		123.3	3 203 500
	123.3	5 894 800		116.8	6 050 500
	134.4	7 360 852		123.1	7 360 852
	142.6	7 360 852		116.7	7 680 852
	133.0	7 370 852			
				117.0	8 962 752
	132.8	8 962 752			

Figure 16 LB4-1034-2-1  
Fatigue Test Result-±27% Shear Strain

(Sheet 3 Of 3)

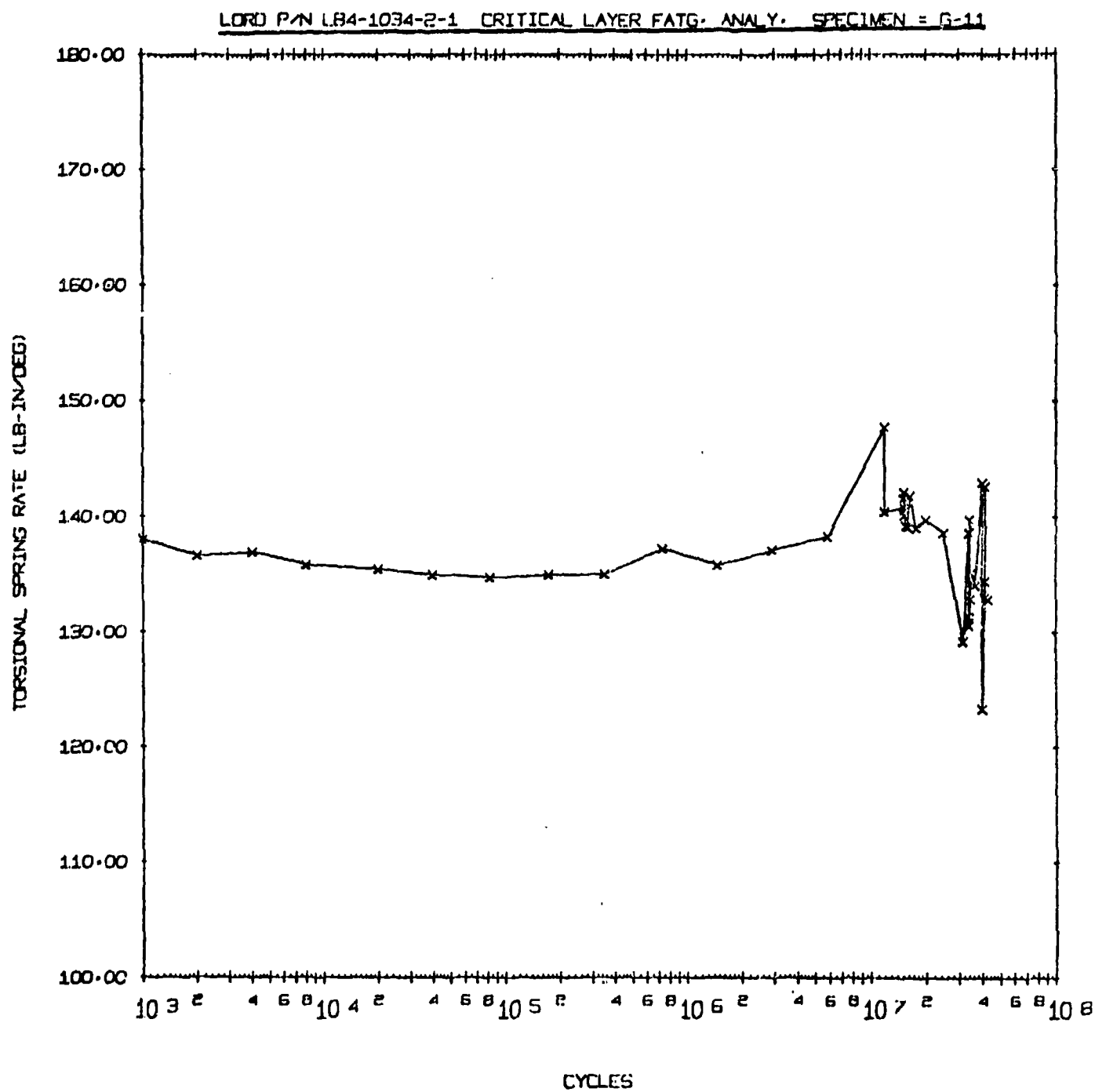


Figure 17

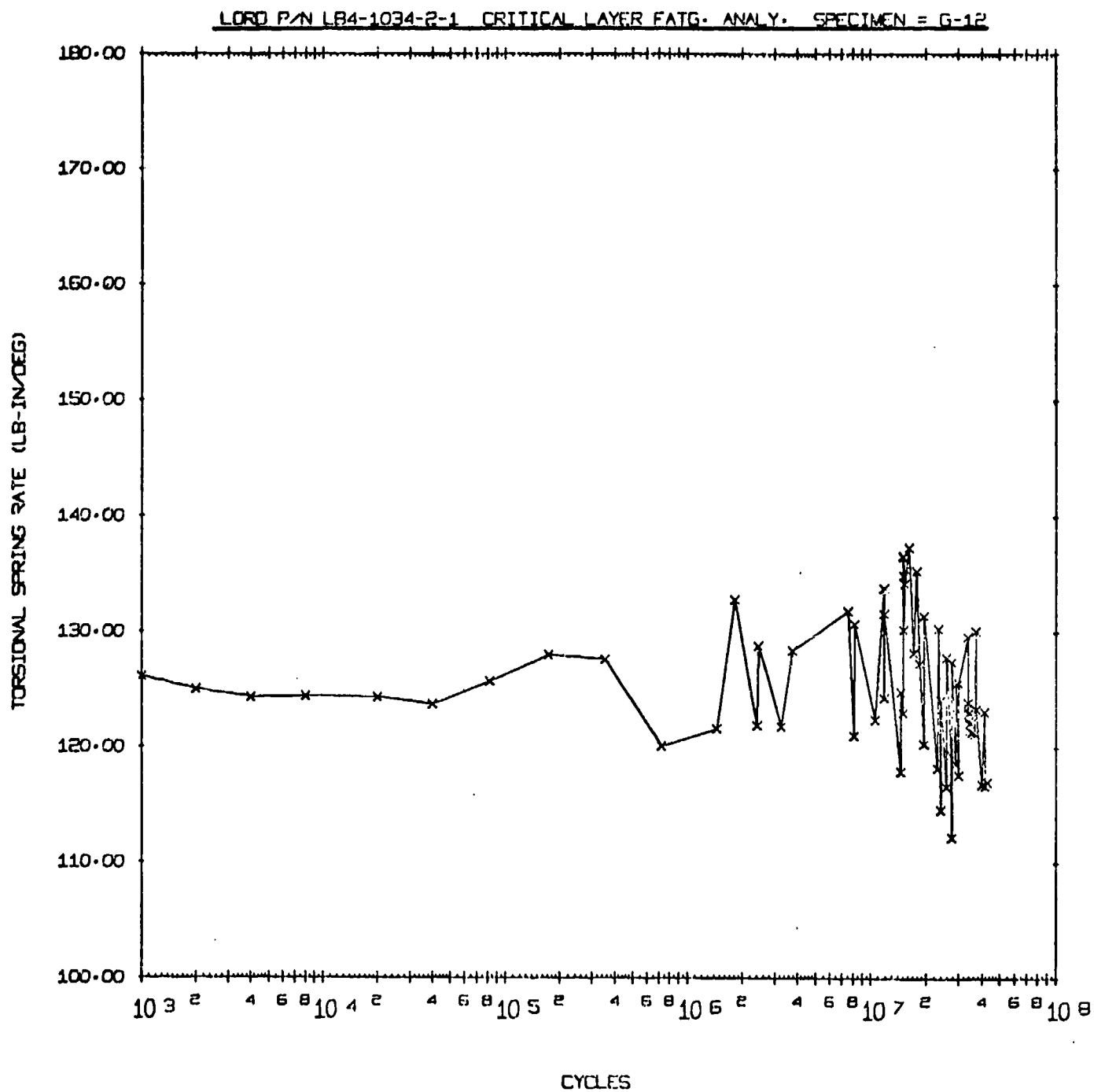


Figure 18



STATION # 2  
PART# TL367-1-5

INPUT CONDITIONS- TORSION: .00+- 3.13  
COMPRESSION: 23520.+-

SAMPLE #:	WEST		EAST	
	0- 7		0- 8	
STATUS:	OFF		OFF	
TEST STARTED:	14:59	6 NOV 78	14:59	6 NOV 78
LAST READING:	19:13	7 NOV 78	18:30	8 NOV 78
	(LB-IN/DEG)	(#CYCLES)	(LB-IN/DEG)	(#CYCLES)
REFERENCE:	199.3	0	196.2	0
	195.8	1 000	189.3	1 000
	197.6	2 000	190.8	2 000
	198.3	4 000	190.8	4 000
	197.9	8 000	190.8	8 000
	199.5	20 300	192.4	20 300
	198.8	50 300	193.1	50 300
	199.0	110 300	192.2	110 300
	199.5	230 300	193.9	230 300
	195.5	470 300	193.8	470 300
	184.9	550 300	183.6	660 300
	174.4	620 300	211.1	700 300
	161.8	670 300	183.4	710 300
			173.4	773 800
	155.8	700 300	163.2	863 900
			152.9	923 900
			150.1	933 900

Figure 19 LB5-1034-1-1  
Fatigue Test Result-±110% Shear Strain

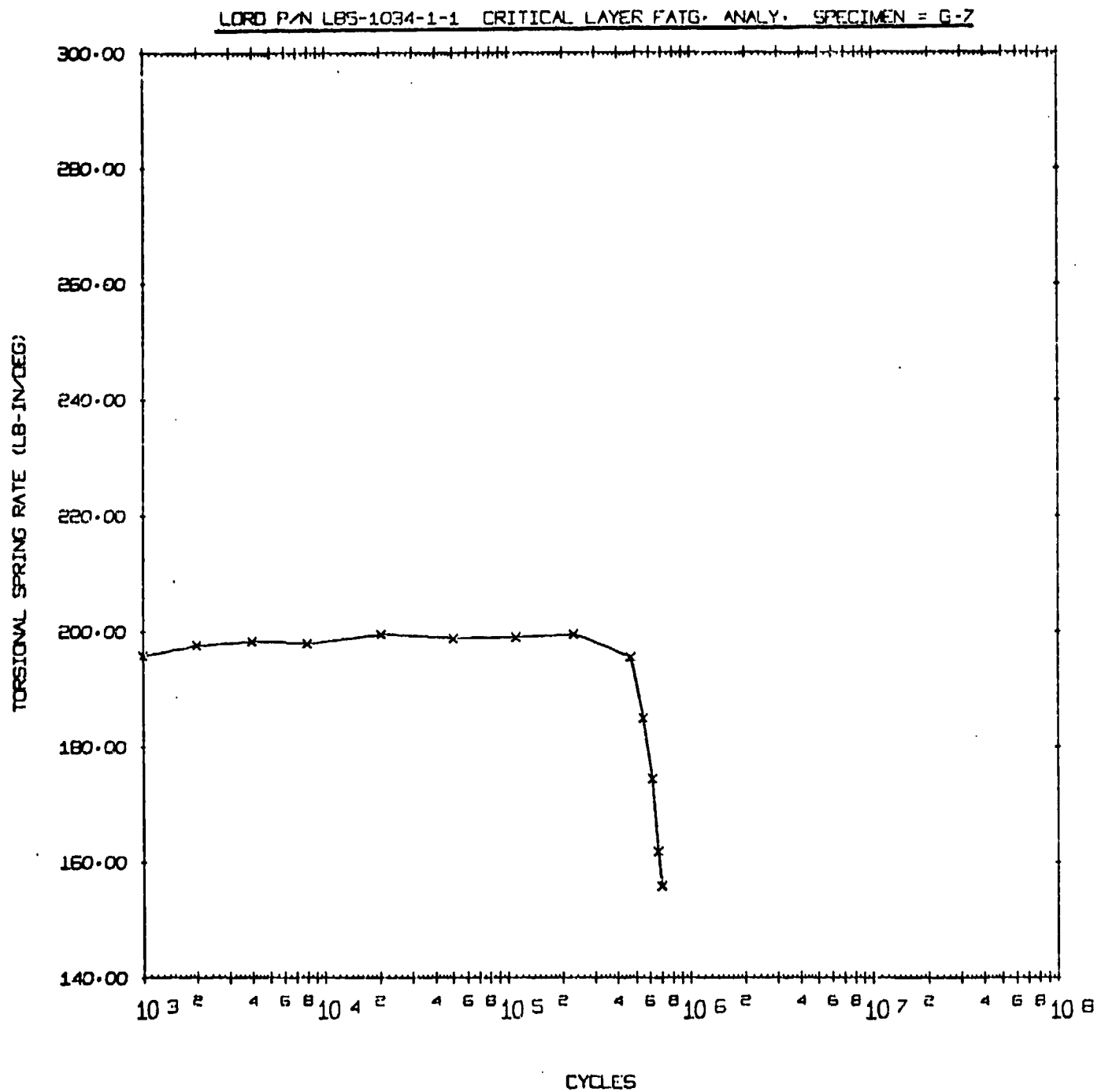


Figure 20

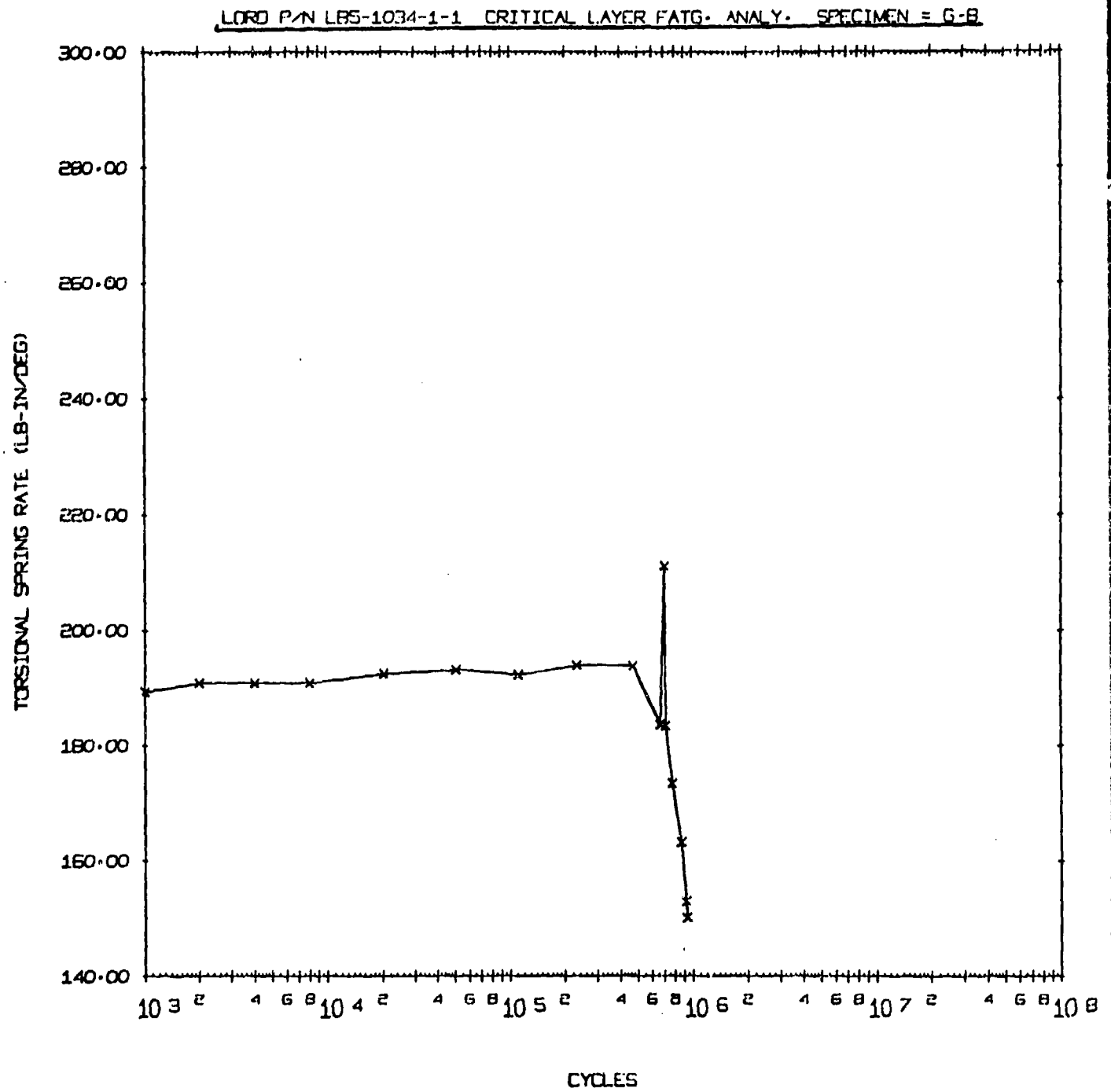


Figure 21

STATION # 2  
PART# TL367-1-5

INPUT CONDITIONS- TORSION: .00+- 2.00  
COMPRESSION: 23520. +-

SAMPLE #: WEST  
STATUS: G- 15  
OFF

EAST  
G- 16  
OFF

TEST STARTED: 13:46 10 NOV 78  
LAST READING: 11:53 17 NOV 78

13:46 10 NOV 78  
18:50 20 NOV 78

	(LB-IN/DEG)	(#CYCLES)		(LB-IN/DEG)	(#CYCLES)
REFERENCE:	228.2	0		225.4	0
	211.4	1 000		205.1	1 000
	211.2	2 000		205.8	2 000
	210.8	4 000		205.2	4 000
	210.9	8 000		204.5	8 000
	210.3	16 000		203.7	16 000
	213.0	39 000		205.7	39 000
	212.6	79 000		204.4	79 000
	214.0	159 000		206.8	159 000
	214.0	319 000		206.9	319 000
	215.2	639 000		208.5	639 000
	211.9	1 279 000		213.0	1 279 000
	228.8	1 387 800		228.2	1 387 800
	214.1	1 397 800		214.8	1 397 800
	200.7	1 777 800		227.7	2 464 200
	214.1	2 464 200		211.4	2 474 200
	199.2	2 474 200		194.9	2 987 600
	188.2	2 774 200		206.5	2 997 600
	177.6	2 957 600		196.0	4 147 600
				184.9	4 617 600
	168.5	3 527 600		174.4	5 107 600
				162.7	5 453 200
				162.7	5 453 200

Figure 22 LB5-1034-1-1  
Fatigue Test Result-±70% Shear Strain

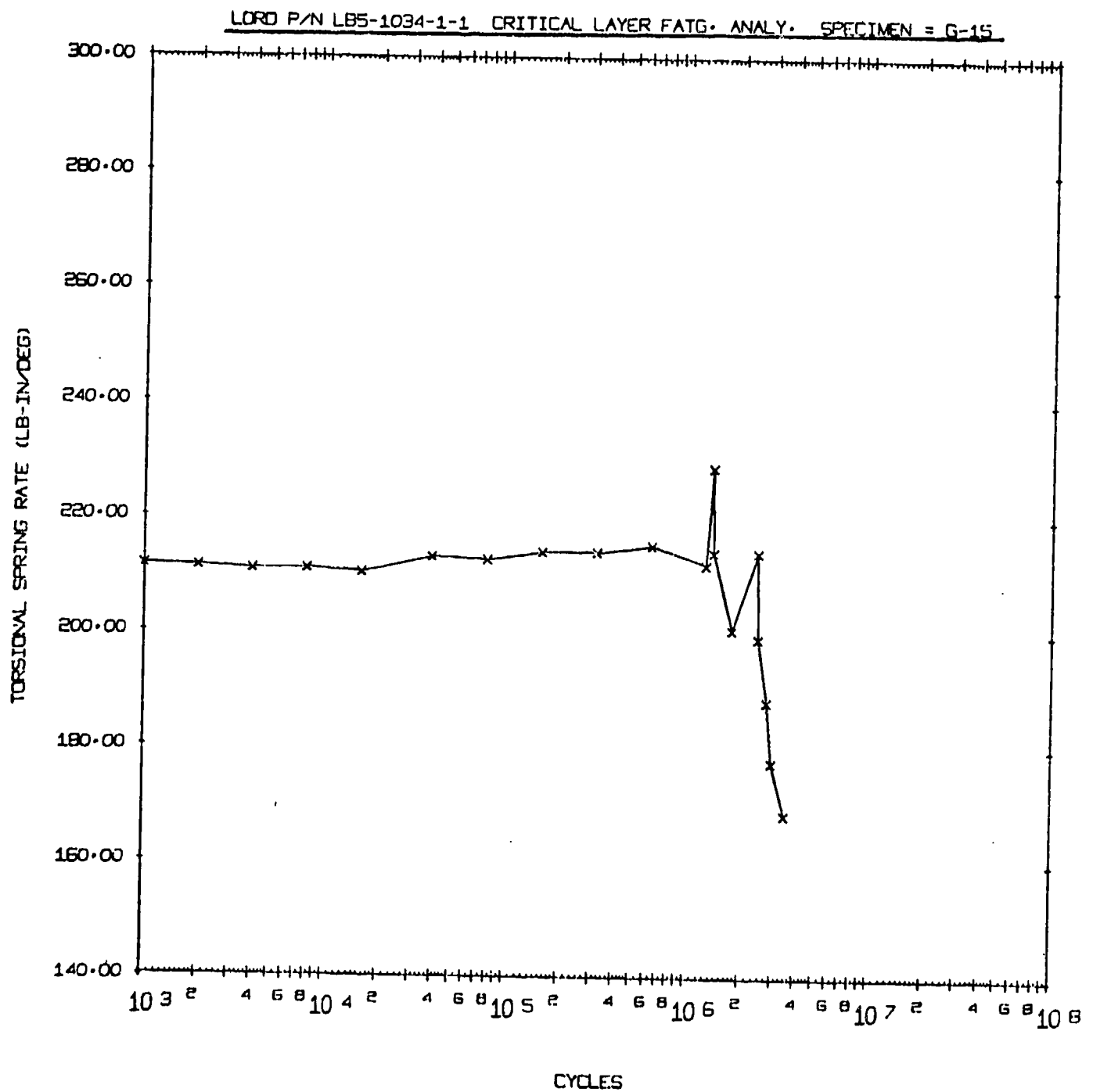


Figure 23

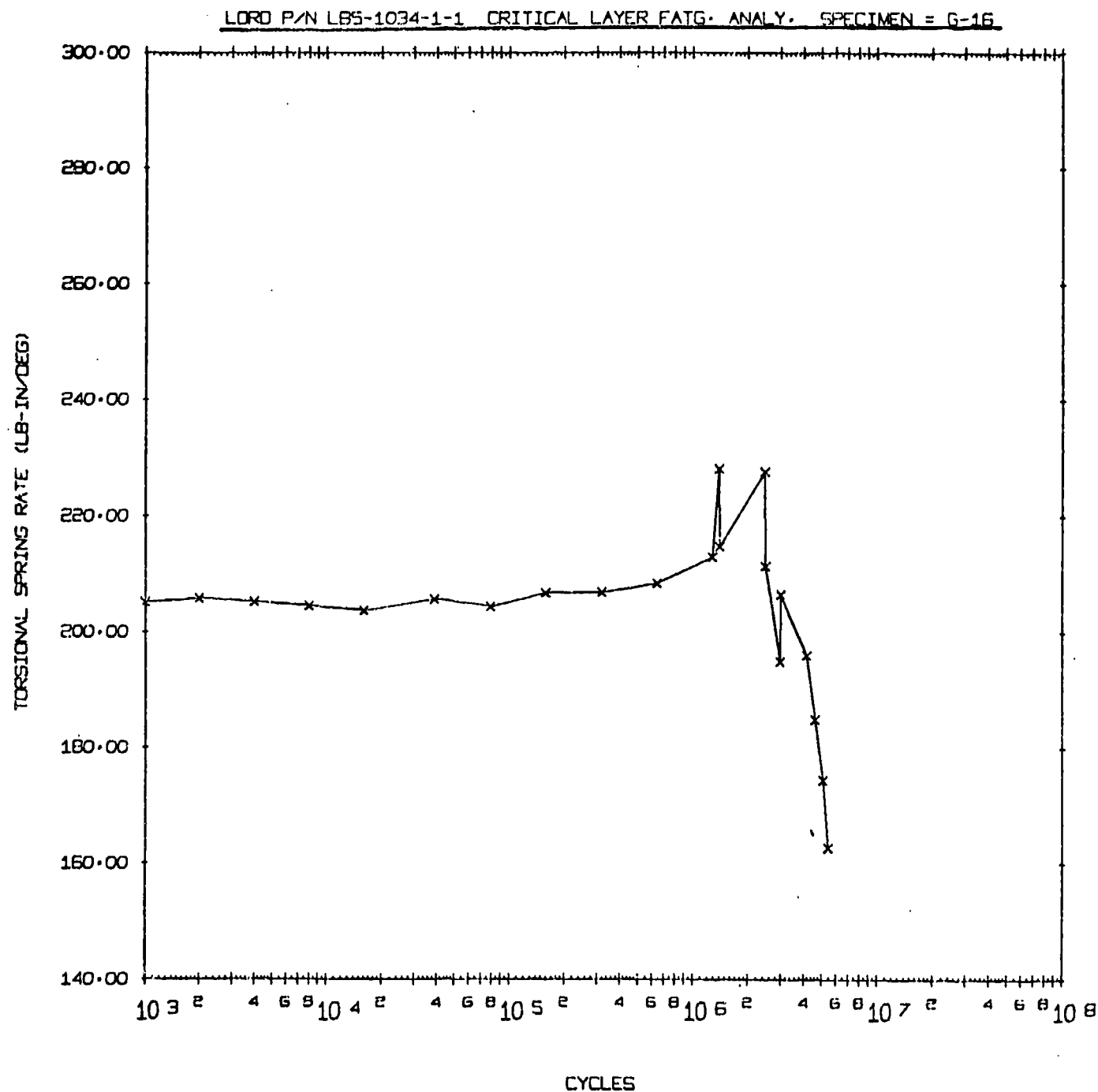


Figure 24.

STATION # 2  
PART# TL367-1-5

INPUT CONDITIONS- TORSION: .00+- 1.00  
COMPRESSION: 23520. +-

SAMPLE #: WEST EAST  
STATUS: G- 17 15T G- 18  
HOLD HOLD

TEST STARTED: 10:57 16 JUN 79 10:57 16 JUN 79  
LAST READING: 16:15 27 JUL 79 16:15 27 JUL 79

	(LB-IN/DEG)	(#CYCLES)		(LB-IN/DEG)	(#CYCLES)
	237.8	0		233.8	0
REFERENCE:	222.2	1 000		217.5	1 000
	220.4	2 000		215.7	2 000
	221.5	4 000		216.3	4 000
	221.6	8 000		216.0	8 000
	224.2	20 000		218.6	20 000
	226.3	40 000		220.4	40 000
	223.8	82 400		218.9	82 400
	223.3	172 400		217.8	172 400
	227.1	352 400		221.9	352 400
	223.6	720 897		222.4	720 897
	235.6	1 390 997		226.2	1 450 997
	222.2	1 826 497		228.8	2 910 197
	233.7	1 876 497		246.2	2 950 197
	238.9	3 760 497		234.9	3 070 197
	240.6	7 524 597		249.3	4 700 497
	227.0	10 697 497		234.3	4 830 497
	245.7	10 700 297		230.0	9 666 197
	264.9	11 853 609		217.1	10 697 497
	253.0	11 853 609		235.3	11 853 609
	235.2	11 854 609		224.3	11 853 609
	254.0	12 250 209		213.0	13 810 009
	242.8	13 225 109			
	260.7	13 480 009		214.5	15 085 309
	249.0	13 570 009			
	248.4	15 085 309			

Figure 25. LB5-1034-1-1  
Fatigue Test Results -  $\pm 36\%$  Shear Strain

STATION # 2  
PART# TL367-1-5

INPUT CONDITIONS- TORSION: .00+- 1.00  
COMPRESSION: 23520. +-

SAMPLE #: WEST EAST  
STATUS: 0- 17 2nd File 0- 18  
OFF OFF

TEST STARTED: 10:14 30 JUL 79 10:14 30 JUL 79  
LAST READING: 0 38 20 SEP 79 21:35 3 SEP 79

	(LB-IN/DEG)	(#CYCLES)		(LB-IN/DEG)	(#CYCLES)
REFERENCE.	259.3	0		217.3	0
	254.5	10 000		214.4	10 000
	255.3	30 100		217.3	30 100
	248.4	70 100		215.6	70 100
	247.5	144 000		217.1	144 000
	243.7	294 000		215.0	294 000
	243.6	594 000		213.6	594 000
	243.6	1 194 000		214.8	1 194 000
	246.2	2 388 100		209.6	2 388 100
	248.2	4 780 000		204.1	4 780 000
	242.5	9 568 600		193.2	8 292 800
	236.1	16 602 000		182.2	12 328 700
	239.3	16 612 000		197.9	16 602 000
	236.5	19 429 000		182.8	16 612 000
	244.2	21 915 600		172.0	18 061 700
	226.9	21 925 600			
	275.1	21 971 300		171.4	18 711 700
	236.5	21 971 300			
	223.2	22 072 100			
	210.3	24 763 400			
	203.4	25 573 400			

Figure 25 - LB5-1034-1-1

Fatigue Test Results - ±36% Shear Strain

(Sheet 2 Of 3)



STATION # 2  
PART# TL367-1-5

INPUT CONDITIONS-      TORSION: .00+- 1.00  
COMPRESSION: 23520.+-

SAMPLE #:      WEST      *3RD File*      EAST  
STATUS:      G- 17           G- 18  
                 HOLD           OFF

TEST STARTED: 11:40 20 SEP 79  
LAST READING: 11:22 24 SEP 79

	(LB-IN/DEG)	(#CYCLES)	(LB-IN/DEG)	(#CYCLES)
	224.0	0		
REFERENCE:	226.5	10 000		
	213.1	20 000		
	212.6	40 000		
	207.3	602 436		
	233.3	602 436		
	214.0	612 436		
	206.9	1 234 536		
	204.7	2 204 336		

Figure 25 - LB5-1034-1-1  
Fatigue Test Results -  $\pm 36\%$  Shear Strain

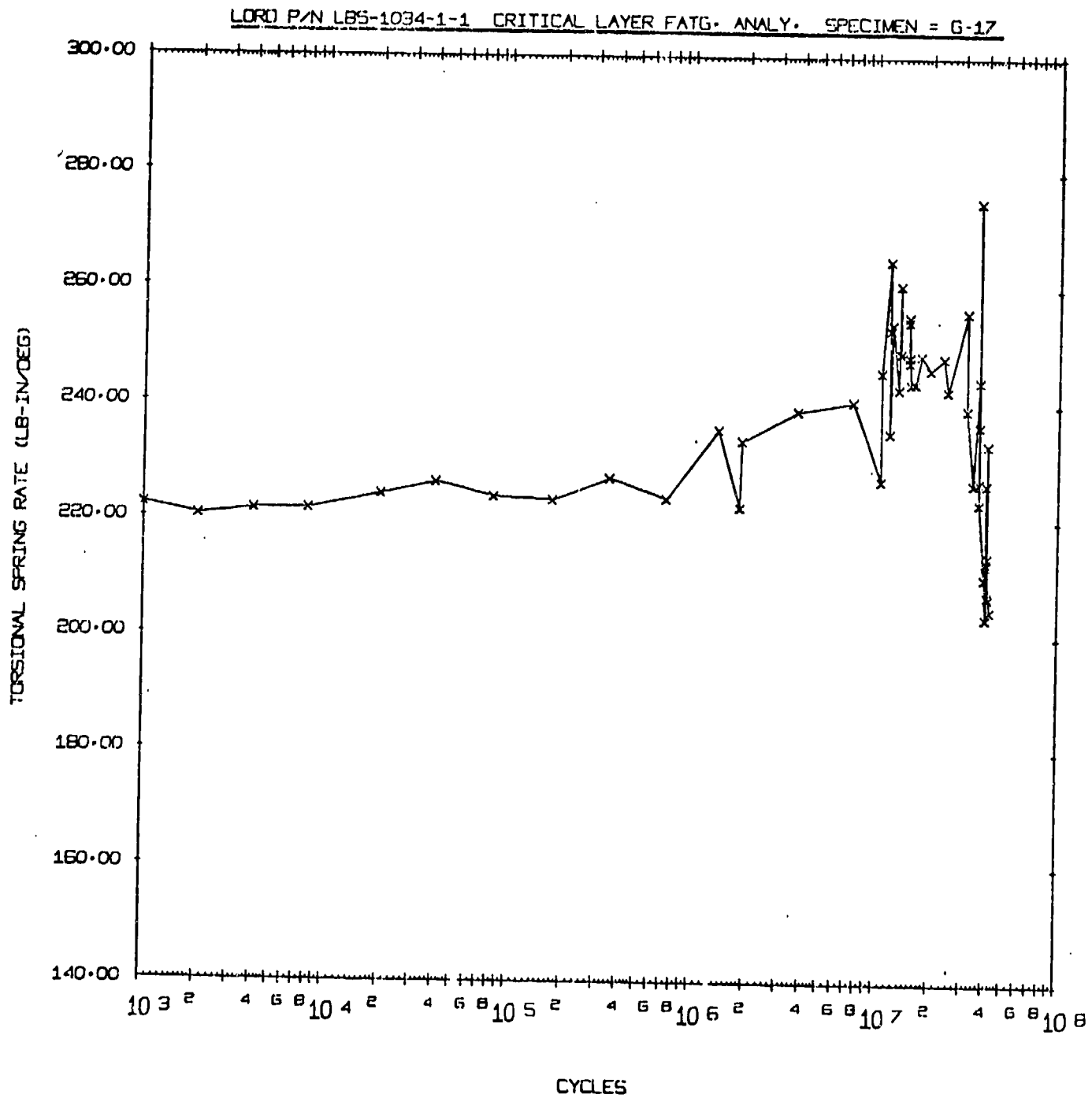


Figure 26

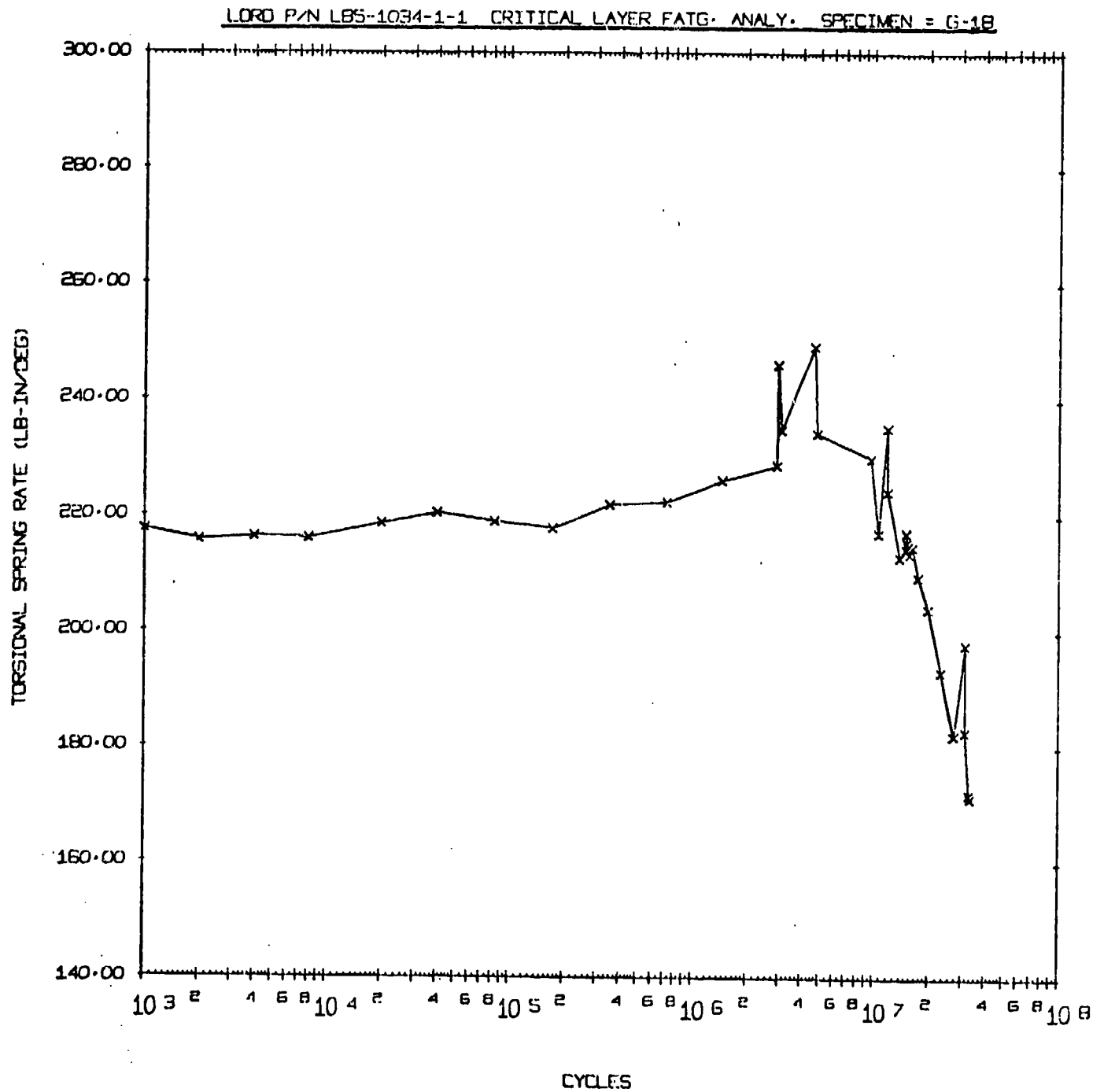


Figure 27



Photograph #25976

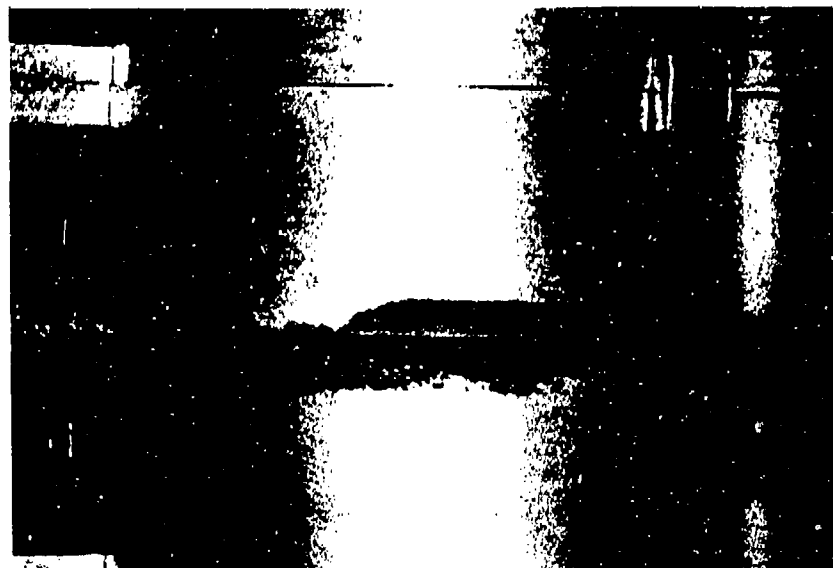
TYPICAL FAILURE APPEARANCE OF TEST SPECIMENS  
DURING S-N CURVE TESTING

AMMRC Contract DAAG46-78-C0030  
Final Report APE79-021



Photograph #26082

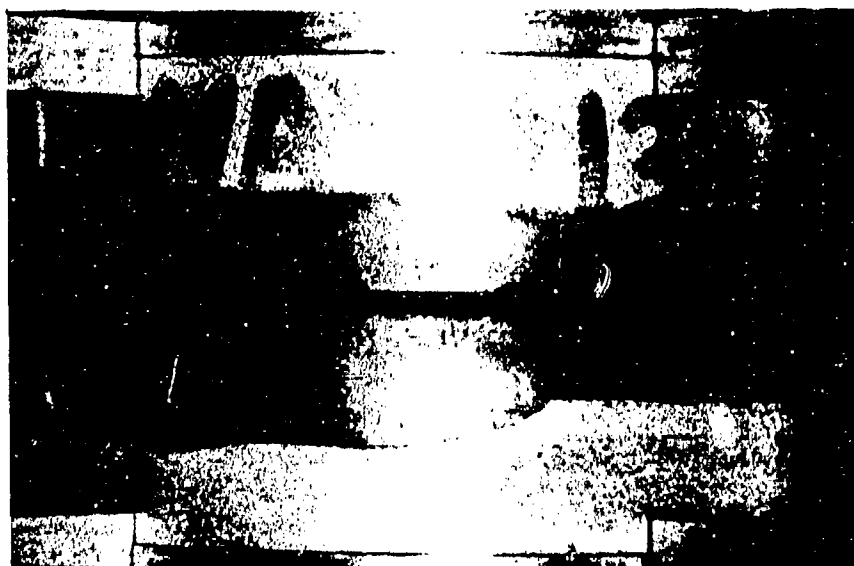
TEST SPECIMEN G-11 (Part not failed)



Photograph #26083

TEST SPECIMEN G-12 (Part not failed)

AMMRC Contract DAAG46-78-C0030  
Final Report APE79-021



Photograph #26084

TEST SPECIMEN G-17 (Part not failed)

### Test Results Comments

The peaks and valleys visible on the plotted data are results of temporary test machine stoppage in which the elastomeric specimen "recovered" some of its stiffness, but quickly returned to its original stiffness after the test was restarted. This behavior is typical of elastomers, and results primarily from hysteresis heating of a few degrees in the elastomer which tends to decrease the stiffness. When the strain is removed the elastomer returns to room temperature and becomes slightly stiffer.

### Fatigue Curve Presentation

The individual bearing S-N curves are presented in Figures 28 and 29. The curves are constructed on log-log graph paper with alternating direct shear strain as the ordinate, and cycles to failure as the abscissa. The curves can also be approximated by the equation:

$$N = \left[ \frac{C}{E_s} \right]^x \quad (2)$$

where

- N = Cycles to failure
- $E_s$  = Alternating direct shear strain, %
- C&x = Constants particular to the given curve, and determined by curve fit methods

The Least Squares curve fit method was used to determine the constants, which resulted in an approximate fit for the LB4-1034-2-1 curve and a very good fit for the LB5-1034-1-1 curve. The equations and their accuracy at the three test points are presented in Table 5. The Least Squares curve for each bearing is included in the S-N curves, Figures 28 and 29.

TABLE 5  
S-N Curve Equations

LB4-1034-2-1

Least Squares Curve Fit Constants

N = Predicted cycles to failure  
s = Shear strain in per cent  
C = 53900  
x = 2.341

Equation:

$$N = \frac{53900}{s^{2.341}}$$

s	Test Cycles to Failure	N @ s	Variance - %
+ 100%	1765250	2481290	+ 40.6
+ 60%	14303000	8203463	- 42.6
+ 27%	42760101	53189600	+ 24.4

LB5-1034-1-1

Least Squares Curve Fit Constants

N = Predicted Cycles to Failure  
s = Shear strain in per cent  
C = 5929  
x = 3.429

Equation:

$$N = \frac{5929}{s^{3.429}}$$

s	Test Cycles to Failure	N @ s	Variance - %
+ 110%	817100	866199	+ 6.0%
+ 70%	4490400	4080480	- 9.1%
+ 36%	38330027	39901766	+ 4.1%



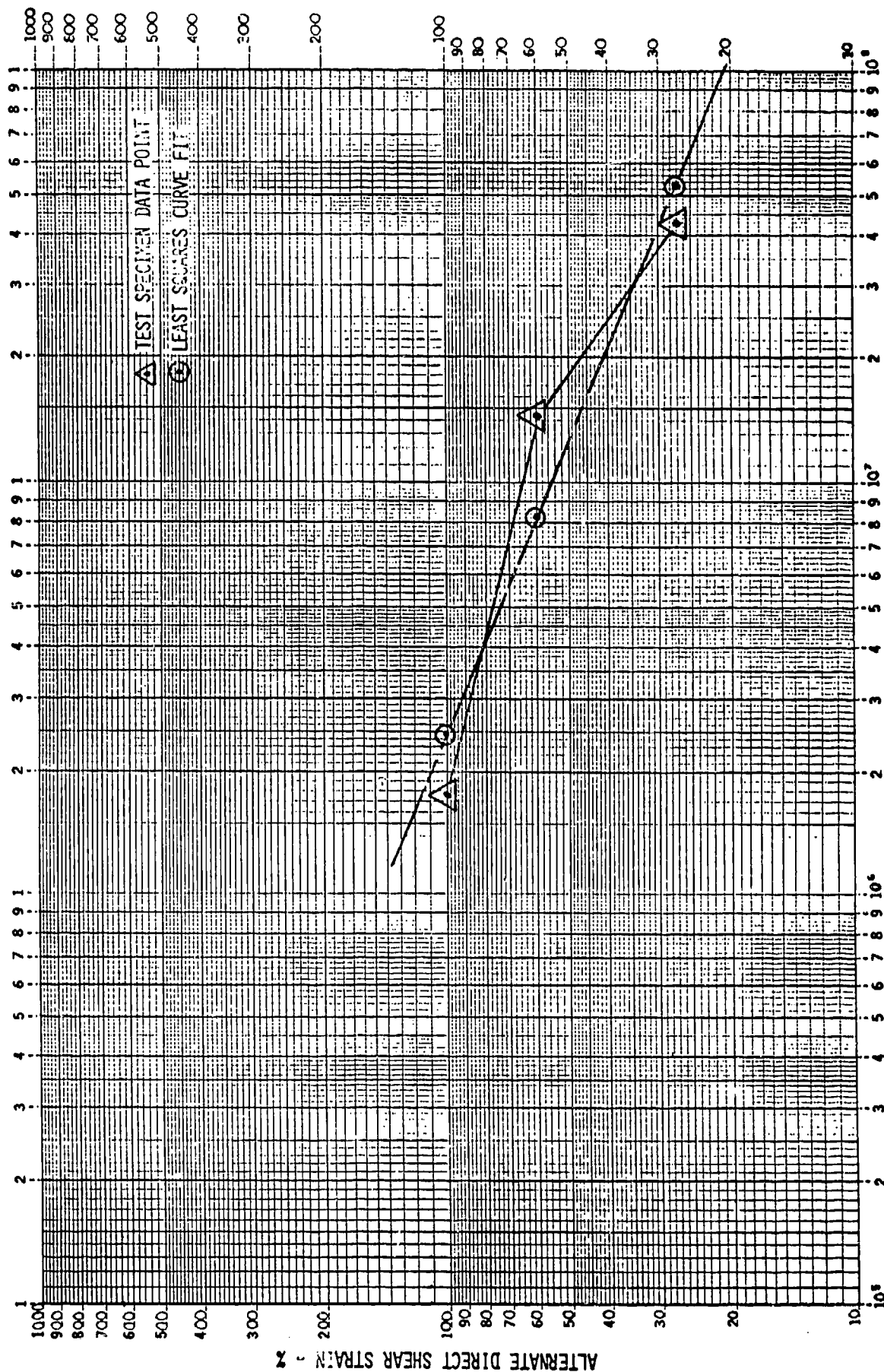


FIGURE 28 LB4-1034-2-1; CRITICAL LAYER S-N CURVE  
LAYER NO. - 17TH FROM FOCAL POINT.

ELASTOMER - MAD 008  
CURVE NO. - C-4952

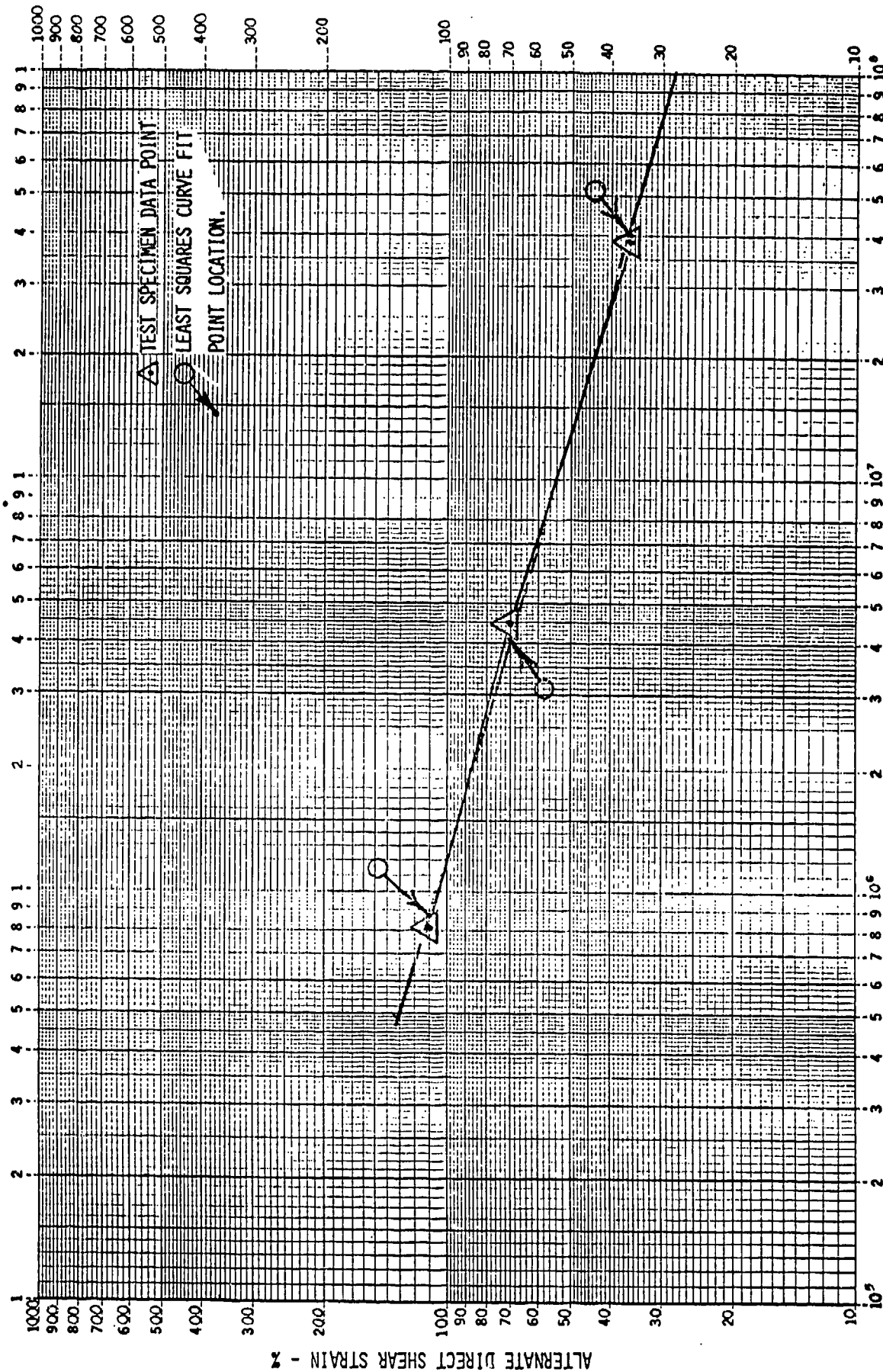


FIGURE 29, LBS-134-1-1; CRITICAL LAYER S-N CURVE  
LAYER NO. - 1ST FROM SMALL END PLATE

ELASTOMER - MAD 013  
CURVE NO. - C-4953

### Life Prediction

Service life prediction was based on the Sikorsky Endurance Loads/Motion Spectrum, SES701059 Rev. 4 dated 4/4/77.

Each condition of SES701059 was used to determine a ratio equal to the expected cycles to failure, using the developed fatigue curves, divided by the number of cycles imposed during a specified lifetime. When the summation of these damage ratios is equal to one, the number of cycles will equal the predicted life.

The damage ratios for the LB4-1034-2-1 bearing were computed using the actual S-N curve as shown in Figure 28. The equation was not used due to its high variance from test results. The damage ratios for the LB5-1034-1-1 bearing were all computed from the Least Squares equation. The equation exhibited a close correlation to the test results and provided a means to calculate damage ratios beyond  $10^8$  cycles, into which category many of the spectrum conditions fell. Table 6 provides a listing of the damage ratio by spectrum condition for each bearing.

AMMRC Contract DAAG46-78-C0030  
Final Report APE79-021

TABLE 6

Service Life Prediction

Design Life: 2000 hrs. @ 258 cpm =  $3.096 \times 10^7$  cycles

LB4-1034-2-1 Direct shear strain per degree (a)  
= 5.68% @ 17th layer from focal point

LB5-1034-1-1 Direct shear strain per degree (a)  
= 2.87% @ 1st layer from small end plate

Cond.	% Time	Req'd. No. of Cycles $\times 10^5$	Altern. Torsional Angle Degrees	LB4-1034-2-1		LB5-1034-1-1	
				Alterna- ting Direct Shear Strain %	Damage Ratio	Alterna- ting Direct Shear Strain %	Damage Ratio
1	.9072	2.809	2.20	12.50	.00312	6.31	.00002
2	.6067	1.878	2.00	11.36	.00190	5.74	.000009
3	1.2135	3.757	1.20	6.82	(b)	3.44	.000003
4	1.2135	3.757	1.90	10.79	(b)	5.45	.000015
5	1.6656	5.157	2.60	14.77	.00670	7.46	.000059
6	1.8173	5.626	3.40	19.31	.00938	9.76	.000160
7	6.0673	18.784	4.30	24.42	.03913	12.34	.001977
8	9.0665	28.070	5.30	30.10	.07291	15.21	.003666
9	4.5505	14.088	6.20	35.22	.04335	17.79	.003149
10	1.5111	4.678	8.30	47.14	.02079	23.82	.002845
11	.9072	2.809	2.20	12.50	.00312	6.31	.000018
12	.6067	1.878	2.00	11.36	.00190	5.74	.000009
13	1.2135	3.757	1.90	10.79	(b)	5.45	.000015
14	1.2135	3.757	2.60	14.77	.00670	7.46	.000043
15	1.6656	5.157	3.50	19.88	.00874	10.05	.000163
16	1.8173	5.626	4.30	24.42	.01172	12.34	.000359
17	6.0673	18.784	5.20	29.54	.04816	14.92	.002297
18	9.0665	28.070	6.10	34.65	.08506	17.51	.005942
19	4.5505	14.088	7.10	40.33	.05031	20.38	.005018
20	1.5111	4.678	9.10	51.688	.02599	26.12	.003902

AMMRC Contract DAAG46-78-C0030  
Final Report APE79-021

Cond.	% Time	Req'd. No. of Cycles x 10 <sup>5</sup>	Altern. Torsional Angle Degrees	LB4-1034-2-1		LB5-1034-1-1	
				Alternating Direct Shear Strain %	Damage Ratio	Alternating Direct Shear Strain %	Damage Ratio
21	.4536	1.404	3.90	22.15	.00273	11.19	.000064
22	.3034	.939	4.30	24.42	.00196	12.34	.000060
23	.6067	1.878	2.90	16.47	.00268	8.32	.000031
24	.6067	1.878	3.00	17.04	.00280	8.61	.000035
25	.8328	2.578	3.80	21.58	.00477	10.91	.000108
26	.9087	2.813	4.90	27.83	.00662	14.06	.000281
27	3.0337	9.392	5.90	33.51	.02722	16.93	.001771
28	4.5333	14.035	7.00	39.76	.05013	20.09	.004760
29	2.2752	7.044	8.00	45.44	.02997	22.96	.003776
30	.7555	2.339	10.10	57.37	.01509	28.99	.002789
31	1.5500	4.799	5.20	29.54	.01231	14.92	.000587
32	3.0000	9.288	1.86	10.56	(b)	5.34	.000034
33	1.0000	3.096	4.47	25.39	.00666	12.83	.000226
34	.7500	2.322	7.14	40.56	.00844	20.49	.000843
35	.7500	2.322	3.76	21.36	(b)	10.79	.000093
36	1.3350	4.133	6.49	36.86	.01333	18.63	.001082
37	3.0580	9.468	7.36	41.80	.03573	21.12	.003811
38	2.3240	7.195	9.04	51.35	.03787	25.94	.005861
39	4.1980	12.997	5.05	28.68	.03170	14.49	.001437
40	.665	2.059	2.10	11.93	.00219	6.03	.000011
41	.0001	.0003	14.40	81.79	.00001	41.33	.000001
42	.0002	.0006	13.50	76.68	.00001	38.75	.000002
43	.0004	.0012	12.50	71.00	.00001	35.88	.000003
44	.0023	.0071	11.50	65.32	.00006	33.01	.000013
45	.0050	.0155	10.50	59.64	.00011	30.14	.000021
46	.0220	.0681	9.50	53.96	.00038	27.27	.000066
47	.1000	.310	8.50	48.28	.00148	24.40	.000205
48	.1100	.341	8.00	45.44	.00145	22.96	.000183
49	.3000	.929	7.50	42.60	.00364	21.53	.000399
50	.6100	1.889	7.00	39.76	.00675	20.09	.000641
51	1.308	4.050	6.50	36.92	.01286	18.66	.001066
52	.0001	.0003	14.40	81.79	.00001	41.33	.000001
53	.0019	.00588	12.60	71.57	.00007	36.16	.000015
54	.0280	.00867	10.90	61.91	.00006	31.28	.000013
55	.1200	.376	10.00	56.80	.00243	28.70	.000433
56	.3900	1.207	9.10	51.69	.00635	26.12	.001007
57	1.5600	4.830	8.20	46.58	.02147	23.53	.002816
58	5.7640	17.845	7.30	41.46	.06734	20.95	.006987
TOTALS					.85567		.071201

- (a) - From original bearing analysis
- (b) - Indicated results extend beyond  $10^8$  cycles.

Predicted life of LB4-1034-2-1 for compression  $\pm$  torsional shear

$$\text{Life} = 2000 \text{ hrs.} / .85567 = 2337 \text{ hours}$$

Predicted life of LB5-1034-1-1 for compression  $\pm$  torsional shear

$$\text{Life} = 2000 \text{ hrs.} / .071201 = 28089 \text{ hours*}$$

\*The original bearing design was optimized for torsional shear rate.

The comparison between the laboratory test specimen life prediction results and the original design analysis life prediction is given in Table 7.

TABLE 7

Comparison of Life Predictions between the Laboratory Test  
Specimen and the Original Design Analysis

<u>Bearing</u>	<u>Damage Ratio Lab. Test Specimen</u>	<u>Damage Ratio Original Analysis</u>
LB4-1034-2-1	.85567	.9062
LB5-1034-1-1	.071201	.058189

### MINER'S CUMULATIVE DAMAGE THEORY TEST

Miner's Cumulative Damage Theory states that failure will occur when the sum of the damage ratios due to a spectrum of load (or motion) conditions is equal to one. In order to verify the validity of Miner's Law, a spectrum of conditions derived from SES701059 was applied to two laboratory specimens to determine the actual fatigue life for comparison with the predicted life. The number of conditions in the Sikorsky spectrum was reduced by combining all torsional shear motions which had approximately the same magnitude. This method gave a compact spectrum which was representative of the actual spectrum in terms of varying degrees of shear motion occurring for different lengths of time in the bearing's life cycle.

The LB5-1034-1-1 bearing specimen was chosen for the test. To achieve a reasonable test time of approximately 120 hours at 7 Hz or  $3.02 \times 10^6$  cycles, the alternating direct shear strain was increased by a factor of six. The change effectively raised the shear strain from approximately 13% to 80%. This modification would not affect the demonstration of the theory, only the point of failure. Table 8 presents the spectrum used with the shear strains and the fatigue life results.

TABLE 8

Miner's Cumulative Damage Theory Test Spectrum

Condition	% Time	Alternating Pitch Motion (Deg.)	Actual Brg. Shear Strains (%)	Test Specimen Shear Strains (%)
1	18.07	4.96	13.0	78.0
2	17.84	5.25	13.7	82.2
3	17.75	5.52	14.3	85.8
4	9.03	4.38	11.3	67.8
5	4.54	7.41	19.3	115.8
6	20.54	4.05	10.6	63.8
7	12.23	4.51	11.8	70.8

TABLE 9

Miner's Cumulative Damage Theory Test Results

Design Test Life = 120 hrs. @ 7 Hz =  $3.024 \times 10^6$  Cycles

(a) Life Prediction per Figure 29

Condition	Required No. of Cycles % Time	Alternating Direct Shear x 10 <sup>5</sup>	Damage Strain %	Ratio
1	18.07	5.483	78.0	.17687
2	17.84	5.413	82.2	.20819
3	17.75	5.386	85.8	.25051
4	9.03	2.749	67.8	.16232
5	4.54	1.228	115.8	.16595
6	20.54	6.229	63.8	.08899
7	12.23	3.716	70.8	.08445
		Total	1.13728	

$$\text{Predicted Failure} = \frac{3.024 \times 10^6 \text{ Cyc.}}{1.13728} = 2.659 \times 10^6 \text{ Cyc.}$$



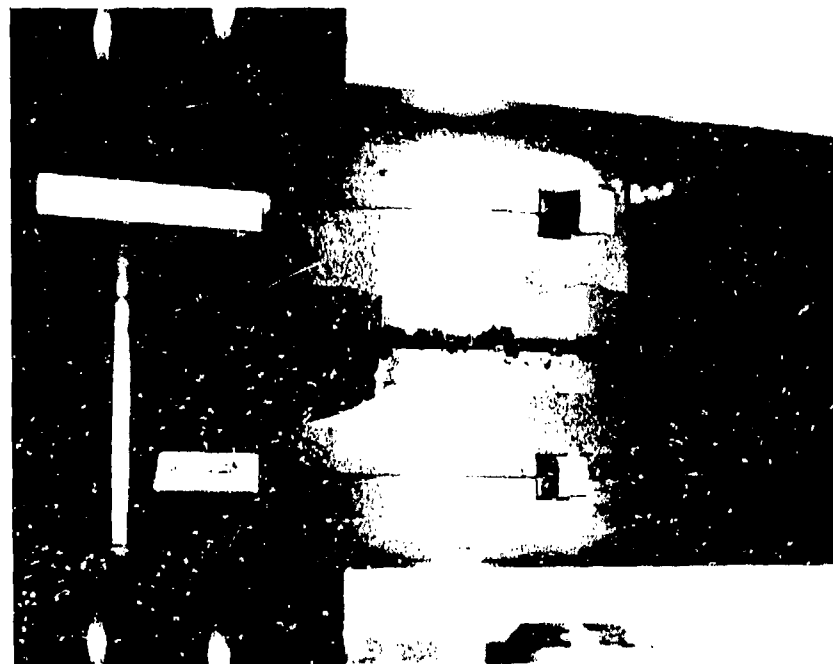
(b) Test Results

Location of Test Specimen on Machine	Test Spec. S/N	Elastomer	Cycles to Failure	Average Cycles to Failure
West	G-2	MAD013	3003200	2743300
East	G-4	MAD013	2483400	

The predicted failure was within 3.2 per cent of the actual test result when considering the average cycles to failure. The indicated results show that Miner's Cumulative Damage Theory is a reliable method for determining the fatigue damage in the UTTAS elastomeric bearings and similar parts.



Photograph # 26176  
MINER'S THEORY TEST SPECIMEN G-4



Photograph #26177  
MINER'S THEORY TEST SPECIMEN G-2

SUMMARY OF CONTRACT REQUIREMENTS AND  
WORK PERFORMED

The following summary lists each of the contract requirements in the same order as they appear in the "Statement of Work" submitted with the Lord Kinematics proposal.

1. The geometry of both Sikorsky UTTAS elastomeric main rotor bearings were modelled, and the appropriate material properties specified for each bearing component. The individual models for each bearing are shown in Figures 2 and 4.
2. A finite element computer analysis was performed utilizing the models generated in Step 1 above. The Lord Kinematics' computer program "SARLAS" was used to conduct the analysis. The actual analysis was done during the initial bearing design with the results used for this test program.
3. The critical elastomer layers of the Sikorsky bearings were determined in terms of direct and indirect shear strains. The LB4-1034-2-1 spherical bearing's critical layer was the 17th from the spherical focal point. The LB5-1034-1-1 thrust bearing's critical layer was the 1st from the small end plate. The direct shear strains were varied to produce the required S-N curve.
4. The stress level in each metal shim was evaluated for both bearings using a combination of finite element analysis, strain gage data, and parametric analysis. The results of the spherical shim analysis were presented as Figure 5. The results of the thrust shim analysis were presented on a Sikorsky mean  $-3\sigma$  S-N curve, shown as Figure 6.

5. The stresses and strains in the critical elastomer layer of each Sikorsky bearing were modelled in a standard Lord Kinematics test specimen (Lord Part Number TL-367), using finite element techniques. The results of the test specimen modelling are shown in Figures 8 and 9 for both Sikorsky bearings.
6. The test specimens were manufactured using the same elastomer, adhesive, and bonding procedures as were used in the respective Sikorsky bearings.
7. The laboratory specimen test conditions were selected to provide the same compression edge shear strain as in the bearing critical layer, while selecting a range of torsional shear inputs to determine the S-N fatigue curve. The test spectrum for each bearing was presented as Table 2. An existing Lord Kinematics test machine (E-297) was used to perform the test. The machine parameters are listed in Table 3.
8. The resulting fatigue data was analyzed and a S-N fatigue curve generated for each of the two Sikorsky bearings. The tabulated data was presented as Table 4 in the text. The spherical bearing (LB4-1034-2-1) S-N curve is given as Figure 28, and the thrust bearing (LB5-1034-1-1) S-N curve is given as Figure 29. The fatigue data is also presented as a Least Squares curve fit approximation to the data. The constants were calculated, with the results and equations presented in Table 5.
9. The predicted service life was calculated for each of the two Sikorsky bearings based on their respective S-N curves, and the Sikorsky spectrum (SES701054). The predicted service life for P/N LB4-1034-2-1 is 2337 hours which compares favorably to a required life of 2000 hours. The predicted life of P/N LB5-1034-1-1 is 28089 hours which has no comparison to the required life of 2000 hours. The latter design had been optimized for shear spring rate to obtain desired bearing performance.

10. A test was conducted to verify that Miner's Cumulative Damage Theory was a valid method in predicting elastomeric life. A spectrum of conditions was derived from the Sikorsky spectrum (SES701059) and applied to two laboratory specimens to determine an actual fatigue life. This life was compared to the predicted life calculated from the appropriate elastomeric S-N curve. Tables 8 and 9 presented the test spectrum and test results respectively.
11. A frequency verification test was performed to determine the highest frequency at which the testing could be validly done. The test frequencies selected were 10 Hz, 7 Hz, and 4.3 Hz. The selected test frequency was 7 Hz, with all subsequent testing conducted at this frequency.
12. A monthly report was submitted in accordance with contract line number 0001AA, and DD Form 1423, sequence number A001.
13. This report is the Final Technical Report, submitted in accordance with DI-S-1800 and DD Form 1423.

### CONCLUSIONS

The results of this testing show:

1. There is a correlation indicated between full scale bearing testing and the prediction of an elastomeric bearing fatigue life using finite element analysis with limited laboratory specimen testing. This prediction technique is dependent on accurate modelling of the critical elastomer layer, and reproducing the stresses and strains onto a laboratory test specimen.
2. Miner's Cumulative Damage Theory is a valid premise in predicting elastomeric fatigue life. The average cycles to failure of the laboratory specimens tested was within 3.2 per cent of the predicted failure point.
3. The combination of using laboratory test specimens subjected to the most critical stresses and strains of an elastomeric bearing, along with Miner's Cumulative Damage Theory, provides an effective means to evaluate the service fatigue life of the bearing.
4. This test is only one point and cannot be viewed as universally accurate. It should be recognized that the described method will produce service life predictions for the Lord Kinematics LB4-1034-2-1 (Sikorsky P/N SB-7001-046) and LB5-1034-1-1 (Sikorsky P/N SB-7002-046) only, since the S-N data to be obtained is valid only for Lord Kinematics' materials, adhesive systems, and shims.

5. The test did not consider the effect of low-cycle repeated loading due to Ground-Air-Ground cycling or the effect of maximum load conditions. The bearings must first be designed to withstand G-A-G loading in excess of what is expected so that induced shear does not become a predominant factor in normal flight.
6. Table 20 provides a summary of where the proposed method would be, in terms of accuracy and cost, relative to the more conventional methods.

TABLE 10

Summary of Methods to Predict Service Life

LEVEL OF COST	TYPE OF TEST	LEVEL OF ACCURACY
(HIGHEST)	FLIGHT TEST	(HIGHEST)
C O S T	Real time laboratory tests using actual bearings, load and motion inputs, and environments	
	Real time laboratory tests using actual bearings simulated load and motion inputs, without environments	A C C U R A C Y
	PROPOSED METHOD - Analytical plus limited laboratory tests of specimens	
	DESIGN GUIDE TECHNIQUES (No specimens, no tests)	
(LOWEST)	PARAMETRIC ANALYSIS	(LOWEST)



RECOMMENDATIONS

The proposed method has been shown to be valid in one case, which is not directly applicable to any other case without specific modelling and testing of that case. Therefore, additional work and testing is needed on different configurations of bearings to validate in a general sense the proposed method.

4327A/djr

# DISTRIBUTION LIST

No. of Copies	To
	Commander, U.S. Army Aviation Research and Development Command, P.O. Box 209, St. Louis, Missouri 63166
10	ATTN: DRDAV-EGX
1	DRDAV-D
1	DRDAV-N
	Project Manager, Advanced Attack Helicopter, P.O. Box 209, St. Louis, Missouri 63166
2	ATTN: DRCPM-AAH-TM
1	DRCPM-AAH-TP
	Project Manager, Black Hawk, P.O. Box 209, St. Louis, Missouri 63166
2	ATTN: DRCPM-BH-T
	Project Manager, CH-47 Modernization, P.O. Box 209, St. Louis, Missouri 63166
2	ATTN: DRCPM-CH-47-MT
	Project Manager, Aircraft Survivability Equipment, P.O. Box 209, St. Louis, Missouri 63166
2	ATTN: DRCPM-ASE-TM
	Project Manager, Cobra, P.O. Box 209, St. Louis, Missouri 63166
2	ATTN: DRCPM-CO-T
	Project Manager, Advanced Scout Helicopter, P.O. Box 209, St. Louis, Missouri 63166
2	ATTN: DRCPM-ASH
	Project Manager, Navigation/Control Systems, Fort Monmouth, New Jersey 07703
2	ATTN: DRCPM-NC-TM
	Project Manager, Tactical Airborne Remotely Piloted Vehicle/Drone Systems, P.O. Box 209, St. Louis, Missouri 63166
2	ATTN: DRCPM-RPV
	Commander, U.S. Army Materiel Development and Readiness Command, 5001 Eisenhower Avenue, Alexandria, Virginia 22333
1	ATTN: DRCMT
1	DRCPM
	Director, Applied Technology Laboratory, Research and Technology Laboratories (AVRADCOM), Fort Eustis, Virginia 23604
1	ATTN: DAVDL-ATL-ATS
	Director, Research and Technology Laboratories (AVRADCOM), Moffett Field, California 94035
1	ATTN: DAVDL-AL-D

No. of  
Copies

To

Director, Langley Directorate, U.S. Army Air Mobility Research and  
Development Laboratories (AVRADCOM), Hampton, Virginia 23365  
1 ATTN: DAVDL-LA, Mail Stop 266

Commander, U.S. Army Avionics Research and Development Activity,  
Fort Monmouth, New Jersey 07703  
1 ATTN: DAVAA-O

Director, Lewis Directorate, U.S. Army Air Mobility Research and  
Development Laboratories, 21000 Brockpark Road, Cleveland, Ohio 44135  
1 ATTN: DAVDL-LE

Director, U.S. Army Materials and Mechanics Research Center  
Watertown, Massachusetts 02172  
2 ATTN: DRXMR-PL  
1 DRXMR-PR  
1 DRXMR-PD  
1 DRXMR-AP  
1 DRXMR-PMT  
8 DRXMR-RC, Mr. B. Halpin

Director, U.S. Army Industrial Base Engineering Activity,  
Rock Island Arsenal, Rock Island, Illinois 61299  
2 ATTN: DRXIB-MT

Commander, U.S. Army Troop Support and Aviation Materiel Readiness Command,  
4300 Goodfellow Boulevard, St. Louis, Missouri 63120  
1 ATTN: DPSTS-PLC  
1 DRSTS-ME  
1 DRSTS-DIL

Office of the Under Secretary of Defense for Research and Engineering,  
The Pentagon, Washington, D.C. 20301  
1 ATTN: Dr. L. L. Lehn, Room 3D 1079

12 Commander, Defense Technical Information Center, Cameron Station,  
Alexandria, Virginia 22314

Defense Industrial Resources Office, DIRSO, Dwyer Building, Cameron Station,  
Alexandria, Virginia 22314  
1 ATTN: Mr. C. P. Downer

Headquarters, Department of the Army, Washington, D.C. 20310  
1 ATTN: DAMA-CSS, Dr. J. Bryant  
1 DAMA-PPP, Mr. R. Vawter

Director, Defense Advanced Research Projects Agency, 1400 Wilson Boulevard,  
Arlington, Virginia 22209  
1 ATTN: Dr. A. Bement

No. of  
Copies

To

Commander, U.S. Army Missile Command, Redstone Arsenal, Alabama 35809

- 1 ATTN: DRSMI-ET
- 1 DRSMI-RBLD, Redstone Scientific Information Center
- 1 DRSMI-NSS

Commander, U.S. Army Tank-Automotive Research and Development Command,  
Warren, Michigan 48090

- 1 ATTN: DRDTA-R
- 1 DRDTA-RCKM, Dr. J. Chevalier
- 1 Technical Library

Commander, U.S. Army Tank-Automotive Materiel Readiness Command,  
Warren, Michigan 48090

- 1 ATTN: DRSTA-EB

Commander, U.S. Army Armament Research and Development Command,  
Dover, New Jersey 07801

- 1 ATTN: DRDAR-PML
- 1 Technical Library
- 1 Mr. Harry E. Pebly, Jr., PLASTEC, Director

Commander, U.S. Army Armament Research and Development Command,  
Watervliet, New York 12189

- 1 ATTN: DRDAR-LCB-S
- 1 SARWV-PPI

Commander, U.S. Army Armament Materiel Readiness Command,  
Rock Island, Illinois 61299

- 1 ATTN: DRSAR-IRB
- 1 DRSAR-IMC
- 1 Technical Library

Commander, U.S. Army Foreign Science and Technology Center,  
220 7th Street, N.E., Charlottesville, Virginia 22901

- 1 ATTN: DRXST-SD3

Commander, U.S. Army Electronics Research and Development Command,  
Fort Monmouth, New Jersey 07703

- 1 ATTN: DELET-DS

Commander, U.S. Army Electronics Research and Development Command,  
2800 Powder Mill Road, Adelphi, Maryland 20783

- 1 ATTN: DRDEL-BC

Commander, U.S. Army Depot Systems Command, Chambersburg,  
Pennsylvania 17201

- 1 ATTN: DRSDS-PMI

Commander, U.S. Army Test and Evaluation Command, Aberdeen Proving Ground,  
Maryland 21005

- 1 ATTN: DRSTE-ME

No. of Copies	To
1	Commander, U.S. Army Communications and Electronics Materiel Readiness Command, Fort Monmouth, New Jersey 07703 ATTN: DRSEL-LE-R
1	Commander, U.S. Army Communications Research and Development Command, Fort Monmouth, New Jersey 07703 ATTN: DRDCO-PPA-TP
1	Director, U.S. Army Ballistic Research Laboratory, Aberdeen Proving Ground, Maryland 21005 ATTN: DRDAR-TSB-S (STINFO)
1	Chief of Naval Research, Arlington, Virginia 22217 ATTN: Code 472
1	Headquarters, Naval Material Command, Washington, D.C. 20360 ATTN: Code MAT-042M
1	Headquarters, Naval Air Systems Command, Washington, D.C. 20361 ATTN: Code 5203
1	Headquarters, Naval Sea Systems Command, 1941 Jefferson Davis Highway, Arlington, Virginia 22376 ATTN: Code 035
1	Headquarters, Naval Electronics Systems Command, Washington, D.C. 20360 ATTN: Code 504
1	Director, Naval Material Command, Industrial Resources Detachment, Building 75-2, Naval Base, Philadelphia, Pennsylvania 19112 ATTN: Technical Director
1	Commander, U.S. Air Force Wright Aeronautical Laboratories, Wright-Patterson Air Force Base, Ohio 45433 ATTN: AFWAL/MLTN
1	AFWAL/MLTM
1	AFWAL/MLTE
1	AFWAL/MLTC
1	National Aeronautics and Space Administration, Washington, D.C. 20546 ATTN: AFS--AD, Office of Scientific and Technical Information
1	National Aeronautics and Space Administration, Marshall Space Flight Center, Huntsville, Alabama 35812 ATTN: R. J. Schwinghammer, EH01, Dir., M&P Lab
1	Mr. W. A. Wilson, EH41, Bldg. 4612
1	Metals and Ceramics Information Center, Battelle Columbus Laboratories, 505 King Avenue, Columbus, Ohio 43201

No. of  
Copies

To

Hughes Helicopters-Summa, M/S T-419, Centinella Avenue and Teale Street,  
Culver City, California 90230

1 ATTN: Mr. R. E. Moore, Bldg. 314

Sikorsky Aircraft Division, United Aircraft Corporation, Stratford,  
Connecticut 06497

1 ATTN: Mr. Melvin M. Schwartz, Chief, Manufacturing Technology

Bell Helicopter Textron, Division of Textron, Inc., P.O. Box 482,  
Fort Worth, Texas 76101

1 ATTN: Mr. P. Baumgartner, Chief, Manufacturing Technology

1 Mr. Robert Phinney, Rotor Design Group

Kaman Aerospace Corporation, Bloomfield, Connecticut 06002

1 ATTN: Mr. A. S. Falcone, Chief, Materials Engineering

Boeing Vertol Company, Box 16858, Philadelphia, Pennsylvania 19142

1 ATTN: R. Pinckney, Manufacturing Technology

1 R. Drago, Advanced Drive Systems Technology

Detroit Diesel Allison Division, General Motors Corporation, P.O. Box 894,  
Indianapolis, Indiana 46206

1 ATTN: James E. Knott, General Manager

General Electric Company, 10449 St. Charles Rock Road, St. Ann,  
Missouri 63074

1 ATTN: Mr. H. Franzen

AVCO-Lycoming Corporation, 550 South Main Street, Stratford,  
Connecticut 08497

1 ATTN: Mr. V. Strautman, Manager, Process Technology Laboratory

United Technologies Corporation, Pratt & Whitney Aircraft Division,  
Manufacturing Research and Development, East Hartford, Connecticut 06108

1 ATTN: Mr. Ray Traynor

Grumman Aerospace Corporation, Plant 2, Bethpage, New York 11714

1 ATTN: Richard Cyphers, Manager, Manufacturing Technology

1 Albert Greci, Manufacturing Engineer, Department 231

Lockheed Missiles and Space Company, Inc., Manufacturing Research,  
1111 Lockheed Way, Sunnyvale, California 94088

1 ATTN: H. Dorfman, Research Specialist

Lockheed Missiles and Space Company, Inc., P.O. Box 504, Sunnyvale,  
California 94086

1 ATTN: D. M. Schwartz, Dept. 55-10, Bldg. 572

Barry Controls, 700 Pleasant Street, Watertown, Massachusetts 02172

1 ATTN: R. R. Peterson, Technical Director